INSTITUTO TECNOLÓGICO
Y DE ESTUDIOS SUPERIORES DE OCCIDENTE

Reconocimiento de validez oficial de estudios de nivel superior según acuerdo secretarial 15018, publicado en el Diario Oficial de la Federación el 29 de noviembre de 1976.

Departamento de Electrónica, Sistemas e Informática

DOCTORADO EN CIENCIAS DE LA INGENIERÍA

DETECCIÓN DE ATAQUES EPILÉPTICOS Y APNEA DEL SUEÑO BASADA EN LA CARACTERIZACIÓN DE SEÑAL

Tesis que para obtener el grado de

DOCTOR EN CIENCIAS DE LA INGENIERÍA

presenta: Jesús Guillermo Servín Aguilar

Director de tesis: Dr. Jorge Arturo Pardiñas Mir

Co-director de tesis: Dr. Luis Rizo Domínguez

Tlaquepaque, Jalisco. Febrero de 2019

DOCTOR EN CIENCIAS DE LA INGENIERÍA (2019) ITESO, Tlaquepaque, Jal., México

TÍTULO: **Detección de ataques epilépticos y apnea del sueño basada en la caracterización de señal**

AUTOR: Jesús Guillermo Servín Aguilar
Ingeniero en Electrónica (ITESO, México)
Maestro en Ciencias (UABC campus Mexicali, México)

DIRECTOR DE TESIS: Jorge Arturo Pardiñas Mir
Departamento de Electrónica, Sistemas e Informática, ITESO
Ingeniero en Electrónica (ITESO, México)
Maestro en Electrónica Industrial (ITESO, México)
Doctor en Telecomunicaciones (*Telecom SudParis/Université Pierre et Marie Curie,* Paris, Francia)

NÚMERO DE PÁGINAS: xxiii, 86

ITESO – The Jesuit University of Guadalajara

Department of Electronics, Systems, and Informatics

DOCTORAL PROGRAM IN ENGINEERING SCIENCES

DETECTION OF EPILEPTIC SEIZURE AND SLEEP APNEA BASED ON SIGNAL CHARACTERIZATION

Thesis to obtain the degree of

DOCTOR IN ENGINEERING SCIENCES

Presents: Jesús Guillermo Servín-Aguilar

Thesis Director: Dr. Jorge Arturo Pardiñas-Mir

Thesis Co-director: Dr. Luis Rizo-Domínguez

Tlaquepaque, Jalisco, Mexico
February 2019

PHD IN ENGINEERING SCIENCES (2019) ITESO, Tlaquepaque, Jal., Mexico

TITLE: **Detection of Epileptic Seizure and Sleep Apnea based on Signal Characterization**

AUTHOR: Jesús Guillermo Servín-Aguilar
Bachelor's degree in electronics engineering (ITESO, Mexico)
Master's degree in science (UABC, Mexico)

THESIS DIRECTOR: Jorge Arturo Pardiñas Mir
Department of Electronics, Systems, and Informatics, ITESO
Bachelor's degree in electronics engineering (ITESO, Mexico)
Master's degree in industrial electronics (ITESO, Mexico)
Ph.D. degree in telecommunications engineering (*Telecom SudParis/Université Pierre et Marie Curie*, Paris, France)

NUMBER OF PAGES: xxiii, 86

This thesis is dedicated to:

My wife Mónica del Carmen and my children Ángela Sofía and Jesús Leonardo, whose unconditional love, patience, and support allow me to complete this thesis.

My parents J. Jesús and Mercedes Aurora, for their complete support and their words of encouragement.

My sisters Mercedes Gabriela, Fernanda Paola, Fátima Bernardett, and Mariana Guadalupe, for always being present at all times.

Resumen

Las enfermedades crónicas son la principal causa de muerte en el mundo. Hospitales alrededor del mundo gastan más de 3.3 trillones de dólares atendiendo a pacientes con estos padecimientos, lo que representa una gran carga para solventar estos tratamientos. Tradicionalmente, los signos vitales son obtenidos en hospitales y los resultados son interpretados por médicos que realizan el diagnostico correspondiente. En los últimos años, diferentes sistemas inalámbricos, como las redes de sensores inalámbricos (WSN, por sus siglas en inglés) o las redes de sensores del área del cuerpo (BASN, por sus siglas en inglés) son usados para escanear los signos vitales de forma remota. Esto da la oportunidad a médicos de realizar diagnósticos o ajustar tratamientos a larga distancia. Estos sistemas normalmente necesitan estar conectados y transmitiendo constantemente, lo que demanda energía. Estos dispositivos tienden a ser pequeños, portátiles y energizados con baterías, garantizando el bienestar del paciente. En este trabajo de tesis se estudian algunas soluciones relacionadas con sistemas de monitoreo remoto, considerando principalmente su eficiencia en el consumo de energía. Por ejemplo, se muestra cómo una señal de encefalografía (EEG) puede ser comprimida empleando transformadas de ondeleta o *wavelet*. La señal de EEG proporciona información sobre la actividad del cerebro y ayuda a entender su funcionamiento. Ayuda, por ejemplo, a detectar enfermedades crónicas como la epilepsia. En esta tesis se presenta el desarrollo de un detector de ataques de epilepsia basado en la caracterización de la señal EEG. Otro importante disfuncionamiento de salud es la apnea del sueño, en la cual el paciente deja de respirar por 10 segundos o más mientras duerme. Esto es un problema serio cuando el paciente deja de respirar 300 veces por noche o por más de 5 minutos. El método médico usado comúnmente para detectar la apnea del sueño es el polisomnógrafo, pero éste típicamente se aplica en hospitales. Algunos investigadores han desarrollado el polisomnógrafo portátil para ser usado en casa midiendo el ritmo cardiaco, la saturación de oxígeno, el tono arterial periférico, etc., pero en ambos casos, esto es invasivo y muy incómodo. En este sentido, varias técnicas no invasivas han sido propuestas para detectar la apnea del sueño, como la tecnología *Ultra Wide-Band* (UWB). Estos sistemas permiten medir el movimiento del pecho del paciente y detectar cuando deja de respirar. En la parte final de este trabajo, se presenta un algoritmo eficiente y paramétricamente optimizado para la detección de la apnea del sueño.

Summary

Chronic diseases are the main cause of death worldwide. They implicate an inherent annual cost for the health care global system of around 3.3 trillion dollars in the traditional hospitals sector. In the traditional method to detect a disease, the vital signs of the patient are locally obtained, then the physician interprets the results and makes a diagnosis. Recently, different wireless systems such as wireless sensor networks (WSN) and body area sensor networks (BASN) have been used to scan the vital signs of the patient distantly connected, giving the opportunity to medical doctors to make a diagnosis or adjust a treatment remotely. These systems normally require to be connected and transmit continuously, demanding energy from devices that tend to be small, portable, and energized from batteries, making sure to guaranty the well-being of the patient. In this doctoral dissertation, some general solutions related to remote monitoring systems, considering energy efficiency, are studied. For example, it is shown how a vital signal can be compressed by using wavelet transforms. A very important vital signal studied in this work is the electroencephalography (EEG) signal, which provides information about the brain activity and helps to understand its function. It helps to detect diseases, such as epilepsy. In this dissertation, it is also presented the development of a fast epilepsy seizure detector based on the characterization of the EEG signal. Another important health issue is the sleep apnea, which consists of a breathing pause of 10 seconds or more while the patient is sleeping. A health damage could be considered when the patient stops breathing at least 300 times per night or its duration is around 5 minutes. The polysomnography is a common medical method to diagnose sleep apnea. However, it is typically applied only in hospitals. Some researchers have designed a portable polysomnography to be used at home, which measures the heart rate, oxygen saturation, peripheral arterial tone, etc. However, in both types of polysomnography (hospitals and home), the method is invasive and not comfortable. As an alternative, non-invasive techniques have been proposed to detect sleep apneas, such as the ultra-wide band technique (UWB). UWB signals allow to measure the movement of the patients' chest and then to detect when the breathing stops. In this doctoral thesis dissertation, an efficient and parametrically optimized algorithm to detect the sleep apnea is proposed.

Acknowledgements

The author wants to express his gratitude to God for giving life, understanding, and tools to finish his Ph.D.

The author wishes to express his sincere appreciation to Dr. Jorge Arturo Pardiñas-Mir, professor of the Department of Electronics, Systems, and Informatics at ITESO, for his encouragement, expert guidance, and keen supervision as doctoral thesis director throughout the course of this work. The author offers his gratitude to Dr. Luis Rizo-Dominguez, professor of the Department of Electronics, Systems, and Informatics at ITESO, for his support as doctoral thesis co-director during the development of this work. He also thanks Dr. Arturo Veloz, Dr. Iván Esteban Villalón-Turrubiates, and Dr. José Ernesto Rayas-Sánchez, members of his Ph.D. Thesis Committee, for their interest, assessment, and suggestions.

Special thanks are due to Dr. Muriel Muller and Dr. Ghalid Abib, from Telecom SudParis, for fruitful cooperation and helpful technical discussions.

It is the author's pleasure to acknowledge fruitful collaboration and stimulating discussions with his colleagues: Mario Alberto Peredo-Durán, José Luis Chávez-Hurtado, Michele Brennan, José Maria Valencia-Velasco, Julio César Ortiz, Juan Pablo García-Vázquez, Adán Noe Espinoza, and Hanen Mehrez.

Special acknowledgement to ITESO and Telecom SudParis to provide the facilities, equipment, and software to successfully complete the Ph.D. studies.

The author gratefully acknowledges the financial assistance through a scholarship granted by the *Consejo Nacional de Ciencia y Tecnología* (CONACYT), Mexican Government, as well as the financial support provided by a grant.

Finally, special thanks are due to my family: my wife Mónica del Carmen and my children Ángela Sofía and Jesús Leonardo, my parents J. Jesús and Mercedes Aurora, my sisters Mercedes Gabriela, Fernanda Paola, Fátima Bernardett, and Mariana Guadalupe, for their understanding, patience, and continuous loving support.

Contenido

Contents

List of Figures

List of Tables

Introduction

Chronic diseases represent the 60% of deaths in the world [WHO-14], which means that patients must be frequently attending hospitals to be treated. As the number of patients in hospitals is increased, the health care cost is affected. In US, the annual cost for the health care of patients with chronic diseases amount to 3.3 trillion dollars [CDC-18]. Thus, the medical bills have been unsustainable for traditional hospital infrastructures [Mamaghanin-11].

In the traditional method to detect a disease, the signs of the patient are locally obtained, for example the electrocardiography (ECG) or the electroencephalography (EEG), then the physician interprets the results and makes a diagnosis. Recently, different wireless systems like wireless sensor network (WSN) and body area sensor network (BASN) have been widely studied in order to scan the vital signs of the patient distantly connected, and they are now giving the opportunity to medical doctors to make a diagnosis or adjust a treatment remotely.

These kind of systems normally require to be connected and transmit continuously, demanding energy from devices that tend to be small, portable and running from batteries. This is why it is necessary to design telemonitoring systems based on wireless sensor networks that can work with as little energy as possible to extend battery life time, guarantying the well-being of the patient. In this doctoral dissertation, some general solutions related to remote monitoring systems, considering energy efficiency, are studied.

An example of a vital sign that can be remotely monitored is the EEG signal. It provides information about the brain activity and helps to understand its function. Millions of voltage peaks are produced in the brain, that the electroencephalograph detects and characterizes the brain activity. This signal can be monitored by WSN and BASN based systems, sending the EEG signal to hospitals. In the hospital, the signal is collected and interpreted in order to detect diseases, such as epilepsy, dementia, Alzheimer, etc. [Guyton-11].

The EEG signal can detect a chronic disease as the epilepsy, which affects approximately 50 million people of all ages worldwide. The epilepsy is characterized by seizures, which are involuntary movements of part of the body or the entire body [WHO-18]. The amplitude and frequency of the brain waves are suddenly higher and faster, respectively, than the normal brain activity [Guyton-11]. The first part of this dissertation presents the development of a faster epilepsy

seizure detector based on the characterization of the EEG signal with low computational cost.

Another important health issue considered in this doctoral dissertation is the sleep apnea. This is a syndrome which affects at least 6 % of the adult population [WHO-17]. The sleep apnea is the breathing pause of 10 seconds or more while the patient is sleeping, that is caused by the obstruction of the airways [Guyton-11]. A health damage could be considered when the patient stops breathing at least 300 times per night or its duration is around 5 minutes [AASM-17], [Guyton-11], and [Varady-03].

The polysomnography is the most common medical method to diagnose sleep apnea [AASM-17], [Guyton-11], and [MEDLINE-17]. However, it is applied only in hospitals and it is not comfortable. Then, non-invasive techniques have been proposed in order to detect sleep apneas, as, for example, the ultra-wide band technique (UWB) [Fedele-15]. UWB signals allow to measure the movement of the patients' chest and then to detect when the breathing stops. In this doctoral dissertation an efficient algorithm to detect the sleep apnea is proposed. This document is organized as follows.

Chapter 1 presents an overview of some general solutions related to remote monitoring systems. In addition, solutions of energy efficiency in remote monitoring system dedicated to health care are shown using data compression as a method to reduce energy consumption.

Chapter 2 provides an alternative to reduce energy consumption using a technique called wavelet transform (WT) to compress the EEG signal. In the chapter, the performance of different wavelet functions to compress the signal are evaluated. Finally, the results are compared with an algorithm taken from the literature (BSBL algorithm).

Chapter 3 shows the features of the EEG signal in an epileptic seizure. The alpha-stable parameters of the EEG signal using different estimators are presented. The distribution of the signal is calculated, and its alpha-stable parameters are captured. Finally, an algorithm which estimates the alpha-stable parameters and detects the epileptic seizures with reduced processing time is designed.

Chapter 4 presents the sleep apnea disorder in a patient. The acquisition of the breathing signal using UWB technology is described. It is shown how the sleep apnea can be automatically detected using the breathing signals and comparative methods. Several experiments are made in order to demonstrate the performance of a simple proposed algorithm.

Chapter 5 explains a new method to detect sleep apnea based on a UWB radar targeting the

sleeping person without previously computing the breathing signal of the patient. The method measures the variance of the UWB received signal. Additionally, some experiments have been made in order to obtain the best values of the detection parameters. The aim is determining the combination of parameters that produces the lowest processing load with the highest correct results.

In the general conclusions, the most relevant remarks about this work are presented and summarized. The overall discussion of the results of the epilepsy seizure and sleep apnea detector are shown. Additionally, some possible future research work based on the results of this doctoral work is proposed.

Finally, Appendix A shows the reference list of the nine internal research reports written during the doctoral studies, and Appendix B shows the list of conference papers published and intellectual property generated as consequence of this work.

1. Low Energy Consumption Monitoring of Vital Signs

Chronic diseases are the leading cause of death in elderly people, and elderly population has increased significantly. Most of these seniors prefer to live alone in their homes, therefore, it is vital to develop reliable and efficient remote monitoring systems to check patient's health continuously. This chapter presents some general solutions related to remote monitoring systems. It also presents solutions in energy efficiency in remote monitoring systems, which are dedicated to health care. Finally, data compression is proposed in order to reduce energy consumption.

1.1. Remote Monitoring of Vital Signs

Benjamin Franklin one day said that "In this world only two things are certain: death and taxes". Death is a fact that is the only true in life. However, it is worrying that the main cause of death in the world are the chronic diseases. In 2008, 60% of deaths in the world were for diseases like diabetes, cancer, heart strokes, etc. [WHO-14]. Mexico is not an exception, because in 2005 diabetes was the leading cause of death. Half of these deaths were for people older than 70 years old [WHO-14]. Moreover, between 2000 and 2050 it is believed that the world population over 60 years will increase from 11% to 22%, which represents 2,000 million of people in the world. This data indicates that the world population has become old [WHO-15]. If we focus on elderly people, we find that most of seniors prefer to live alone in their own homes than to live with their families or in a care center [Huo-09]. The risk is that if they live alone they can have an accident or a health problem caused by their disease and there is no one around to help the patient. So that the time it takes for a family member or medical assistant to know that the elderly has had an accident may be too long and it can cause irreversible damage to patient's health. In fact, most seniors have many health problems, so that ensuring their health opens a new opportunity for electronic devices dedicated to healthcare.

An actual problem around the world is that hospitals have overpopulation of affiliated members and it is very difficult for doctors and hospitals to attend every patient. In Mexico, for

example, where the most important medical institution is the *Instituto Mexicano del Seguro Social* (IMSS) [IMSS-15], with more than 69 millions of people enrolled, physicians attend 485 thousand of patients every day. This is a reason why it is important to design a system to help patients to minimize their number of appointments to the hospital, and help medical doctors to monitor main vital signs of patients from their homes. This will reduce costs and time for both hospitals and patients.

A solution to reduce the number of patients attending hospitals every day is to design a system to monitor vital signs and send the information to a remote database. From there doctors can review, make a diagnosis and give or modify the treatment of a patient via internet. This would be in fact a remote medical appointment [Huo-09].

This situation has represented in the last years a good opportunity for research work aimed to develop solutions in this area. In this scope Wireless Sensor Networks (WSN) and Wireless Body Area Networks (WBAN) have been considered to be applied to monitor patient vital signs constantly (like heart rate, blood pressure, glucose, etc.), as well as the environment parameters (like temperature, humidity, gas, etc.).

In most cases these systems work as follow: the sensors collect data from the body or/and the environment. With the aid of an intermediate device (like a cellphone) data is sent to a remote device to be review by a doctor (remote device like a computer). These computers, which receive the information, are usually located in hospitals so medical experts can review the information, makes a diagnosis, and determine or adjust the corresponding treatment. Finally, the patient can view the diagnosis or new treatment via internet and he can obtain the prescription at the drug store without a hospital visit.

The down side of these systems is that they normally require to be connected and transmitting continuously, demanding energy from devices that tend to be small, portable and running from batteries. In this context, it is necessary to design telemonitoring systems based on wireless sensor networks that can work with as little energy as possible to extend battery life time, guarantying the well-being of the patient.

We consider that it is important to find a way to get control of the patient disease and ensure his welfare, but we need to design an effective method to reduce energy consumption and maintain the reliability of devices in use. We are interested in studying ways to save energy in devices; in the next section, a synthesis of some research work addressing this problem is presented.

1.2. Synthesis of Works Related to Energy Efficiency

In this section, we review previous research of systems for elderly people monitoring. Health telemonitoring systems are an easy way to supervise patient's health for physicians and family members and they offer them a faster assistance in an emergency scenario. These systems usually show the patient vital signs and their environmental live conditions.

Remote telemonitoring systems can be an alternative to monitor patient's vital signs, however, if we want that customers accept these devices, it is necessary to consider three main issues in their designs [Zhang-13c]:

a) Low Energy Consumption, which is necessary to have long life time batteries. It is important also to consider that the devices must have small and light batteries and small sensors, because it will be comfortable for costumers.
b) Data Compression, which is required because usually devices use large data, sensors, and devices need to save energy sending data with minimum length possible. Finally,
c) Hardware Cost, which is important because devices are better accepted by customers when the final cost is not so high.

If we focus on energy consumption, the sum of all energies is a way to know how much energy is consumed by the system [Awad-13]. To reduce energy consumption, we can analyze the energy distribution process. An example is designing an effective compression technique. If we increase compression ratio, then the transmitted data decreases and devices can be put to sleep for more time and save more energy. Another example is designing an effective transmission technique. If we want to transmit information in a wireless channel, it is necessary to characterize the channel to obtain information about the signal to noise ratio, distance between transmitter and receiver, if the devices have a line of sight (LoS), etc. With this information, we can calculate the total required energy to send data and its rate.

Considering the remote telemonitoring system as a way to monitor patient's vital signs, several papers have proposed some solutions. An example is Virtual Caregiver [Hossain-12]. In this article, authors place sensors in the body to sense vital signs such as blood pressure, glucose, body temperature, etc. They also place sensors around the environment to get some external conditions such as humidity, temperature, etc. Firstly, the system determines the patient status, and if parameters are correct, the system sends a record to a remote computer to be stored and reviewed

by a doctor via WiFi or SMS. However, if the system detects an unusual parameter on vital signs or on the environment conditions, it will send an alarm to a family member and the hospital to get a fast assistance.

Another example to telemonitoring vital signs remotely is the ViCare, which is reported in [Huo-09]. This system determines where the patient is located and senses the environment to determinate if it is safe. For example, if the patient is sleeping in his bedroom and the television is on, the system puts off the television after a certain time. Another example is that, if the patient falls down, the system sends an alarm to his Human Caregiver. Depending on the situation the ViCare decides to send an alarm to the patient's Human Caregiver or make an action to solve the problem.

Finally, Cognitive Agents are reported in [Nefti-10], which use sensors around the house (like gas detector, door or window open, water detector, etc.) to determine when a risky event could occur and the position of the patient in the house. For example, if a senior is at the kitchen and after a certain time he decides to go to another room but forgets to put off the stove, one sensor detects the gas and another sensor determines where the senior is, if the senior is not in the kitchen anymore, the system alarm rings to announce the problem for the senior to react and find the cause of the sound. But if the stove is still on after a certain time, the system determines that a risky situation could occur and sends an emergency alarm via WiFi for a quick medical assistance.

Virtual Caregiver, ViCare and Cognitive Agents are systems which need to be running all the time. Some authors proposed to reduce energy consumption by integrating all system components (sensors, filters, modulators, antennas, etc.) in only one device.

An example of this system integration is presented in [Zhang-13a]. It is proposed a scalable monitoring system to get vital signs using an ultra-low power called Advanced and Adaptive Network Technology (ANT). Their approach is a complete system with microprocessor, filters, and sensors. ANT technology can send information via ZigBee or Bluetooth depending on the length of the data.

Another example of a system integration is reported in [Kannan-13]. A wearable device (CC2540) has three different sensors (ECG, EEG, and EMG). The CC2540 sends the information via Bluetooth to another device (OMAP3530). The OMAP3530 processes the data and sends it via WIFI to a remote computer. The computer located at a hospital receives the signal and cancels the noise using morphological filters. Finally, the recovered signal is shown in the doctor's computer

to be interpreted.

Systems like [Zhang-13a] and [Kannan-13] can be an option to reduce energy consumption because the power used to send information between devices (like transmitter, encoder, modulator, etc.) is minimal.

Another alternative to reduce energy consumption regardless of the location of the device in the system, is the compression of the data.

An approach to obtain an efficient energy system with data compression is proposed in [Liu-13], [Zhang-12], [Zhang-13b], and [Zhang-13c]. The objective is to explore the feasibility of using a new data compression model called Block Sparse Bayesian Learning (BSBL). This BSBL works together with an algorithm called Compressed Sensing (CS). Authors said that to obtain a good quality in the recovered signal it is necessary to use both algorithms, which authors reported a similarity of 95 % between recovered signal and original signal.

[Liu-13], [Zhang-12], [Zhang-13b], and [Zhang-13c], authors tested different biomedical signals in their papers. In [Zhang-13b] they used an EEG signal, in [Zhang-13c] they used a Fetal ECG, in [Zhang-12] it is demonstrated that their frameworks have a better performance than other frameworks, finally in [Liu-13] an expansion of their work uses their framework to obtain data from multiple inputs.

A proposal to evaluate the power efficiency of the system is in [Abualsaud-13], [Awad-13], and [Hussein-13]. The goal in these papers is to reduce the energy consumption in mobile nodes at two levels: compression and communication, changing the parameters of the system according to the input signal.

EEG signals are used in [Abualsaud-13], [Awad-13], and [Hussein-13]. In [Abualsaud-13], EEG records by different subjects (healthy and epilepsy disease), are taken to detect when a person has epilepsy. In [Awad-13], some experiments change parameters like distortion and delay deadline to evaluate different algorithms to obtain the best performance between energy, delays and distortion. Finally, in [Hussein-13], a system is presented, which changes its energy consumption according to channel variations.

In short, new technologies are looking to get good performance with low cost and low energy consumption in its devices. Algorithms, frameworks, and electronic tablets are designed to provide the patient the guarantee that his device has a long battery life time and a good quality signal. It is important to determine how we can obtain an efficient energy consumption in our

devices. Among the different forms to achieve this objective, in our case we consider that data compression is an interesting opportunity to study in our research work and apply it in a wireless sensor area network.

1.3. Conclusions

We have identified many research works on WSN and/or WBAN for healthcare applications. These networks are designed to work all the time and it is necessary to design an efficient energy consumption to extend battery life time, ensuring that the received signal is equal to the original signal.

There are many ways to save energy in a WSN. We can identify the opportunity of research contributions by studying compression techniques to obtain this energy efficiency. It is important to consider that if we want to send more information with less energy, we need to design an effective model of compression techniques.

We found that signals used in health related research works in energy efficiency are EEG and ECG, because these signals normally have multiple channels and they are measured constantly.

2. Compression of Electroencephalographic Signals using Wavelets

Different seizures can be detected with long-term monitoring. Wavelet transform (WT) is an important technique to detect seizures for non-stationary signals, such as ECG or EEG. WT uses the wavelet function to change its bandwidth scaling for time and amplitude. Different waveforms can be used as a wavelet function; a scaled set of these waveforms are called families. In this chapter, we evaluate the performance of different wavelet functions to compress EEG signals. Our results are compared to a combined algorithm (Block Sparse Bayesian Learning and Compressed Sensing).

2.1. Electroencephalographic Signals

Electroencephalography (EEG) signals have been the interest for many contributions in the researched field, which give us the possibility to compare our results and determine the performance of our algorithm. EEG signals give information to understand the brain function and detect diseases, like epilepsy, dementia, Alzheimer, etc. [Guyton-11]. The EEG signals have different frequencies depending on the brain region and the patient status. For example, alpha waves (α) are rhythmic and lie between 8 – 13 Hz, with a typical amplitude of 50 mV. They are present when an adult person is awake and relaxed, and they can be mainly found in the occipital part of the brain. Beta waves (β) lie between 13 and 32 Hz and they are arrhythmic. They can be normally found in the parietal and frontal part of the brain when the patient is awake and performing his daily activities. Theta waves lie between 4 and 7 Hz. They are present in degenerative brain states or many brain disorders. They are located in the parietal and temporal part of the brain in children. Delta waves lie between 0.5 and 3 Hz. They can occur when the patient is in deep sleep. They can present the double of amplitude than the other waves. Finally, Gamma waves lie between 32 and 80 Hz. They are located in the cortex of the brain [Guyton-11]. Finally, Gamma waves lies between 32 and 100 Hz [Marzbani-16]. The brain waves are depicted in Fig. 2.1.

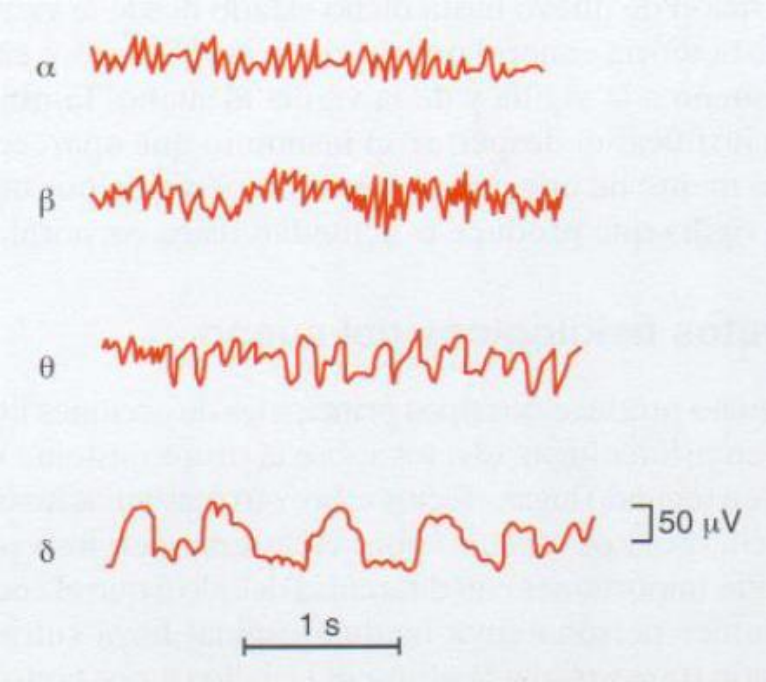

Fig. 2.1 Brain waves alpha, beta, theta, and delta. Figure taken from [Guyton-11].

Then, according to the sampling theorem, it is necessary to have a sampling frequency greater than twice the maximum frequency of the signal. Considering that the maximum frequencies of the brain waves lie around 80 Hz, a good sampling frequency could be 200 Hz. If the signal is quantized at 16 bits/sample in a period of 24 hours, then the collected data length is 34.5 Mbytes per day in a simple channel. However, in [Ramgopal-14] is presented a comparative study of different EEG machines on the market and the maximum number of channels is 40. Considering this traffic information, the amount of data represents 1.38 Gbytes of information per day. The energy used by these devices in transmission presents a big challenge. Motivated by this context, a comparison of different EEG signal compressors reported in the literature is discussed in this chapter.

Different authors have proposed compressor algorithms to reduce the number of samples from the original data and reduce the energy consumption. In [Abualsaud-13], authors design an algorithm which changes the threshold of different blocks of the system (transmitter, modulator, encoder, etc.). The proposed algorithm finds the best performance for every block and it reduces the total energy consumption of the system. Also, pre-designed wavelet Transform (WT) algorithms to compress an EEG signal are presented. In [Perez-Sevilla-97], author used WT to compress an electrocardiography signal (ECG); however, an EEG signal is not considered. In

[Gandhi-11] it is presented an evaluation of wavelet families to detect features of an EEG signal, such as energy, entropy, and standard deviation. Their results show that Coiflets family has a better performance than Haar, Daubechies, and Biorthogonal families, however, this work does not compress the EEG signal. In [Zhang-13b], a combination of a compression techniques called Compressed Sensing (CS) and Block Sparse Bayesian Learning (BSBL) algorithm is presented. The combined compression algorithm is compared to WT using different biomedical signals, such as EEG, ECG, and Fetal EEG. The proposed algorithm in [Zhang-13b] shows low power consumption and a better compression rate for WT.

In summary, the literature shows that WT is a widely used technique to compress EEG signals. WT presents different family's options, for that reason, in this chapter Haar, Daubechies, and Coiflets are evaluated to compress an EEG signal. Our aim in this chapter is to determine which family has the best performance. Therefore, three different criteria are considered: Normalized Mean Square Error (NMSE), Percent of Root-mean-square (PRD), and Compression Ratio (CR).

2.2. Wavelet Transform for Signal Analysis

2.2.1 Wavelet Transform in Discrete Time

It is important to characterize a signal to obtain information about it and, as said before, WT is an alternative to analyze non-stationary signals, such as EEG. The WT relies on signals called windows, which are scaled in amplitude (a) and shifted in time (t).

For the first step, WT equation in discrete time is given by

$$WT(k,a) = \frac{1}{\sqrt{a}} \sum_{n=0}^{\infty} x(n) h\left(\frac{n-k}{a}\right) \tag{2-1}$$

where $x(n)$ is the original signal, h is the wavelet function, n is the sample, a is the scale, $a = 1,2,4,8,...,2^j$, j is a real and positive number, and k is the translation parameter which is a real and positive number.

To recover the signal in discrete time, the inverse wavelet transform is expressed by

$$x(n) = A \frac{1}{\sqrt{2^j}} \sum_{j=0}^{L} \sum_{k=1}^{N-1} WT\left(k, 2^j\right) h\left(\frac{n-k}{2^j}\right) \tag{2-2}$$

where the constant A depends on the wavelet family $h_{j,k}(n)$, and N is the length of the compressed

signal.

An important part of the WT is the wavelet function, because if the scale is changed on the wavelet function, the bandwidth changes and the target signal can be more accurately analyzed. The wavelet function equation is given by:

$$h_{a,k}(n) = \frac{1}{\sqrt{a}} h(\frac{n-k}{a}) \tag{2-3}$$

The variation on *a* implies changes in frequency domain, if *a* increases, then the bandwidth *H*(*w*) decreases. However, if *a* decreases then the bandwidth *H*(*w*) increases. For our work, the dyadic function is considered [Sahambi-97], where the scale $a = 2^j$, and *j* is 1, 2, …, m. When the parameter *j* is small, then the wavelet function will be contracted in time but the amplitude will be greater. In the other way, when a parameter *j* is large, then the wavelet function will be expanded in time but the amplitude will be lower. When the wavelet function is expanded in time, high frequencies of information can be detected. When the wavelet function is contracted in time, low frequencies information can be detected [Perez-Sevilla-97].

The wavelet function requires two admissibility conditions. The first one is given by

$$\int_{-\infty}^{\infty} \frac{|\hat{H}(\varpi)|^2}{|\varpi|} = C_H < \infty \tag{2-4}$$

This equation represents the total sum of all wavelet function components and must be a constant number less than infinite. The second necessary admissibility condition is given by

$$\int_{-\infty}^{\infty} h(t)dt = 0 \tag{2-5}$$

In this case, (2-5) represents the value under the area of the waveform of the wavelet function and must be zero.

When the equations are scaled to form a family, different components of a signal can be obtained using WT and the target signal is analyzed. Fig. 2.2 shows a block diagram of analyzing a signal using WT.

In Fig. 2.2 we see that $x(n)$ is the signal to be analyzed, $h_j(n)$ is the wavelet function which will be scaled in time and frequency to obtain different resolutions. Every scaled wavelet function gives different time-frequency components of the original signal.

Fig. 2.3 shows how the inverse WT works with (2), the synthesis of the target signal. The already analyzed signal can be recovered with the inverse WT. The inverse WT considers the same wavelet function characteristics used to transform the signal. Finally, it is necessary to sum all parts of the signal to recover the original signal.

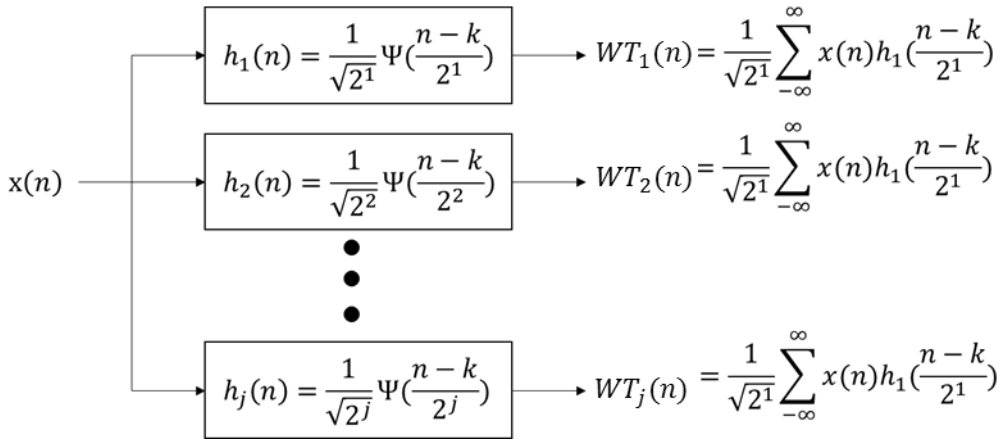

Fig. 2.2 Block diagram of analysis of target signal *x*(*n*).

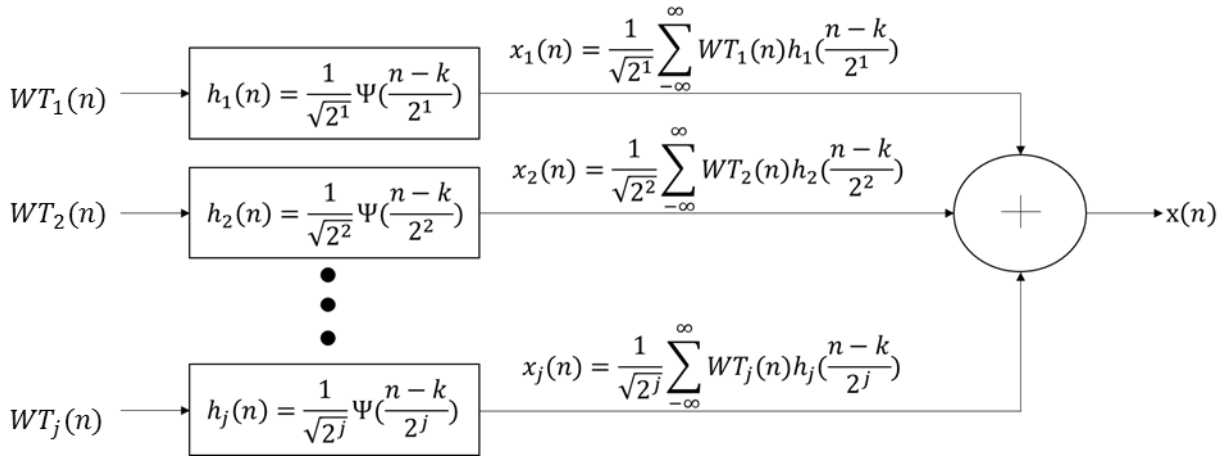

Fig. 2.3 Block diagram of synthesis of signal *x*(*n*).

2.2.2 Wavelet Function Families

2.2.2.1 Haar Family

A wavelet function can create different waveforms which forms a family. Every family has different characteristics which provides different resolution to detect different frequencies in a signal [Mallat-99]. In this section, three different families are studied.

The first family is the Haar function, which obtains a precise approximation if the original signal has smooth variations [Mallat-99]. The Haar function is considered the base family in WT

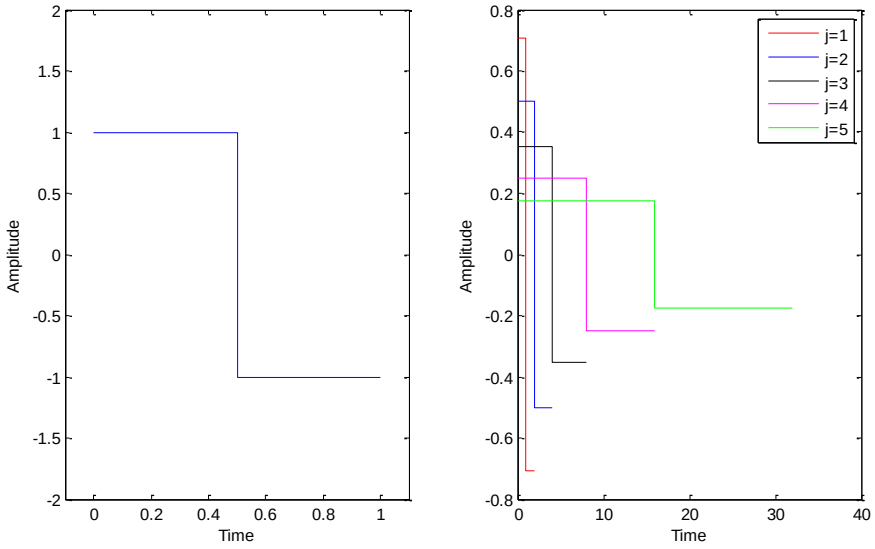

Fig. 2.4 a) Waveform of basic Haar function, b) Waveform of five scaled Haar functions.

and it is expressed by

$$h(n) = \begin{cases} 1 & 0 \le n < 1/2 \\ -1 & 1/2 \le n < 1 \\ 0 & Other \end{cases} \tag{2-6}$$

Fig. 2.4a shows the basic Haar function while Fig. 2.4b shows five Haar functions scaled. Five different scaled functions obtained from 5 values of *j* which are scaled in amplitude and time. Every scaled wavelet function gives a different bandwidth, which extracts different frequency components of the original signal. When the wavelet function has a $j = 1$, the function is contracted in time and rapid changes in time are detected. But when the wavelet function is expanded in time, the signals with low changes in time can be detected.

2.2.2.2 First Derivate of Gaussian Family

The first derivate of the Gaussian function is the base for another wavelet family, which is frequently studied by researchers. This family is used, for example, in computer vision to detect multiscale edges [Sahambi-97]. The equation to represent this wavelet function is given by

$$h(t) = e^{-t^2} \frac{d}{dt} \tag{2-7}$$

The waveform of the first derivate of a Gaussian function is shown in Fig. 2.5a and the waveform of five scaled functions are shown in Fig. 2.5b.

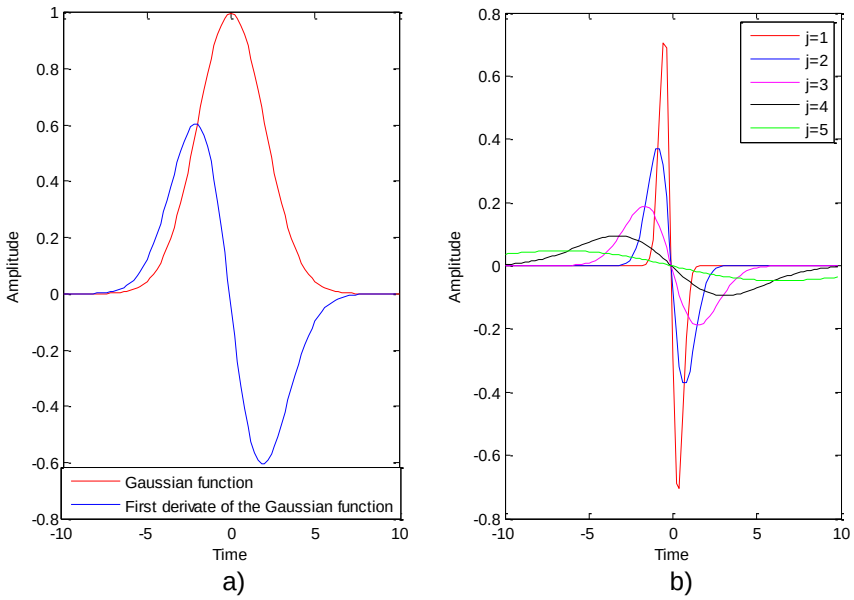

Fig. 2.5 a) Waveform of the first derivate of a Gaussian function, b) Five scaled functions of the first derivate of a Gaussian function.

Like the Haar function, when the parameter *j* is changed, the wavelet function is scaled in time and frequency. By scaling the wavelet function, different windows and different resolutions are obtained to analyze different frequency components of the original signal. The main difference between Haar function and the first derivate of Gaussian function is that the waveform in the first derivate of Gaussian function is centered in zero. Moreover, the waveform of the Haar function begins at zero.

2.2.2.3 Daubechies Family

The Daubechies function is optimal in the sense that they have a minimum size support of a given number of vanishing moments. In this function a pre-design table is used with coefficients depending on the scale of the function, given in [Mallat-99]. When the value of $j = 1$, the Daubechies function is the Haar function [Mallat-99] for that reason the value of *j* must be equal or larger than 2.

In Fig. 2.6a the basic waveform of the Daubechies function is shown and in Fig. 2.6b five scaled Daubechies functions are presented.

Fig. 2.6b shows that the principal positive curve in the waveform is practically the same

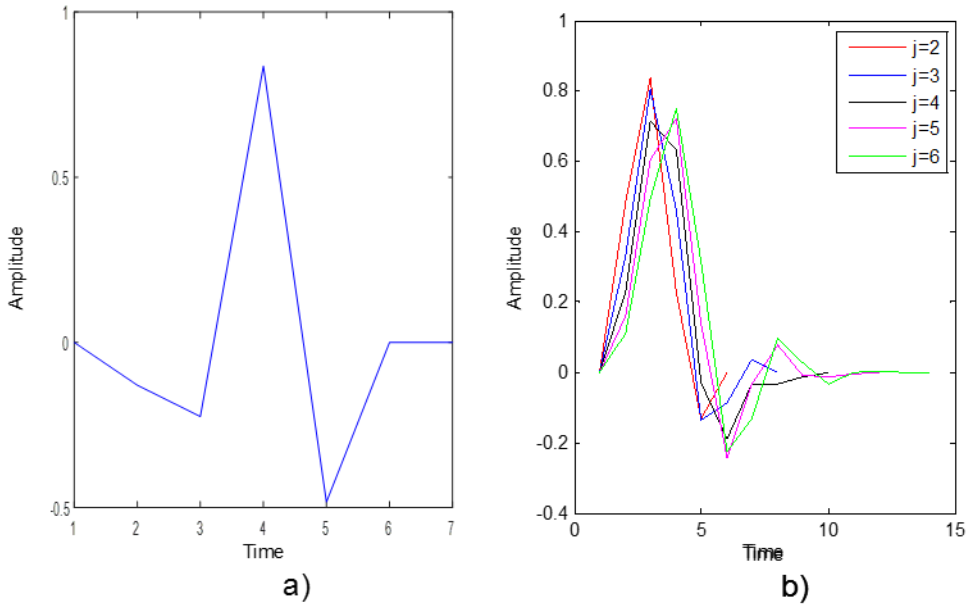

Fig. 2.6 a) Waveform of the basic Daubechies function. b) Five scaled Daubechies functions.

for all members of the family. The difference between members of the family is given by the last part of the waveform, which is expanded when the value of *j* is larger.

2.2.2.4 Spectrum of the Wavelet Functions

In Section II.B, three different families (Haar, First derivate of Gaussian, and Daubechies) were described. However, it is also important to analyze the corresponding spectra. The spectrum gives the bandwidth of every function and it gives the cover frequencies to detect a signal.

Fig. 2.7 shows the spectrum of the three different wavelet functions, which are scaled with different values of *j*. It is seen from Fig. 2.7 that the Haar family covers more frequencies than the other families. For example, when $j = 1$, the Haar family covers almost twice the frequencies than the first derivate of the Gaussian family. However, the amplitude in the first derivate of the Guassian family is larger than the Haar family when $j = 2, 3, 4$, and 5. Finally, Daubechies family has a similar spectrum in the five members of the family. The amplitude and frequencies covered by the five members of the Daubechies family are similar to each one.

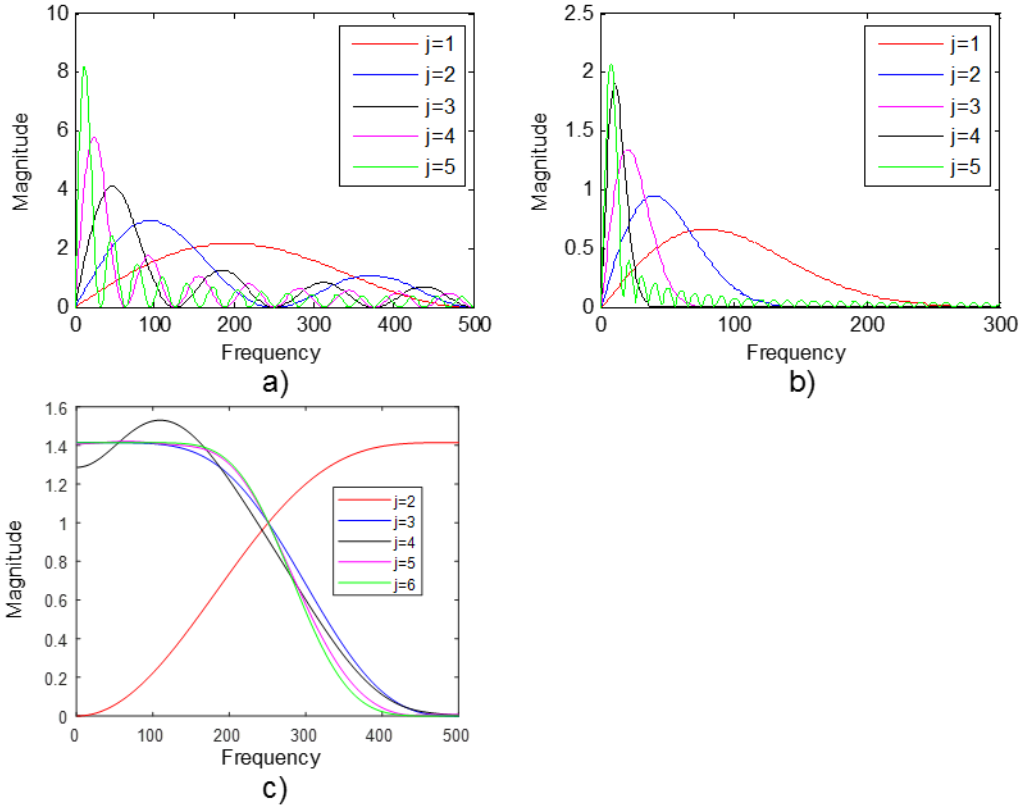

Fig. 2.7 a) Spectrum of the Haar function family, b) Spectrum of the first derivate of Gaussian family, c) Spectrum of the Daubechies family.

2.3. EEG Signals Compression Using Wavelet Transform

2.3.1 Data Compression Using Wavelet Transform

The WT is a widely used technique to compress non-sparse and biomedical signals [Gandhi-11]. WT divides a signal into dilated and translated signal representations in the time/frequency plane. To scale and translate a signal, mother wavelet function varies the parameters of the wavelet function to obtain different time supports [Mallat-99]. The mother wavelet function, called Dyadic wavelet, is given by

$$h_{j,k}(n) = \frac{1}{\sqrt{2^j}} h\left(\frac{n-k}{2^j}\right) \tag{2-8}$$

where j is the scaling parameter, which is a positive number related to a member family, h is the

waveform of a member family, and *k* is the translation parameter, which is a real and positive number. When the value of *j* is low, the WT becomes more sensitive to high-frequency components of the signal, and vice versa [Sahambi-97].

Different waveforms can be generated using wavelet functions, which are called wavelet families. The WT in discrete time is given by

$$WT(k, 2^j) = \frac{1}{\sqrt{2^j}} \sum_{n=0}^{N-1} x(n) h(\frac{n-k}{2^j}) \tag{2-9}$$

where $x(n)$ is the original signal and N is the length of $x(n)$. The inverse WT is used to recover the transformed signal.

The equation of the inverse WT is

$$x(n) = A \frac{1}{\sqrt{2^j}} \sum_{j=0}^{L} \sum_{k=0}^{N-1} WT(k, 2^j)\, h(\frac{n-k}{2^j}) \tag{2-10}$$

where A is a positive number related to amplitude normalization.

According to [Mallat-99], the multiresolution approximation relies on the wavelet function and its corresponding conjugate mirror. When the wavelet function $h(n)$ is analyzed with Fourier Transform, the discrete approximation is a low-pass filtering of the input sampled at intervals of 2^j. Then $h(n)$ is the filter which is associated to low frequencies of the signal. On the other hand, the conjugate mirror filter of $h(n)$, which is given by $g(n)$, contains the high frequencies of the signal [Perez-Sevilla-97]. The relationship between $h(n)$ and $g(n)$ is given by

$$g(n) = (-1)^n h_{-n+1} \tag{2-11}$$

The Mallat algorithm [Perez-Sevilla-97] is an approach to multiresolution approximation which divides the original signal into two transformed signals. The transformed signals have the same length of the original signal [Perez-Sevilla-97]. After that, the two transformed signals are down-sampled; as a result, outcomes present half-length samples from the input. This process can be repeated as many times as needed. Fig. 2.8 illustrates a numerical example of the WT using the Mallat algorithm. Fig. 2.8a shows a signal $x(n)$ composed by 8 samples, which is divided into two parts using WT and the process is repeated one more time. At the end, the transformed signal is composed by four elements which have two samples each one. Finally, Fig. 2.8b shows that the recovered signal is exactly the original signal $x(n)$.

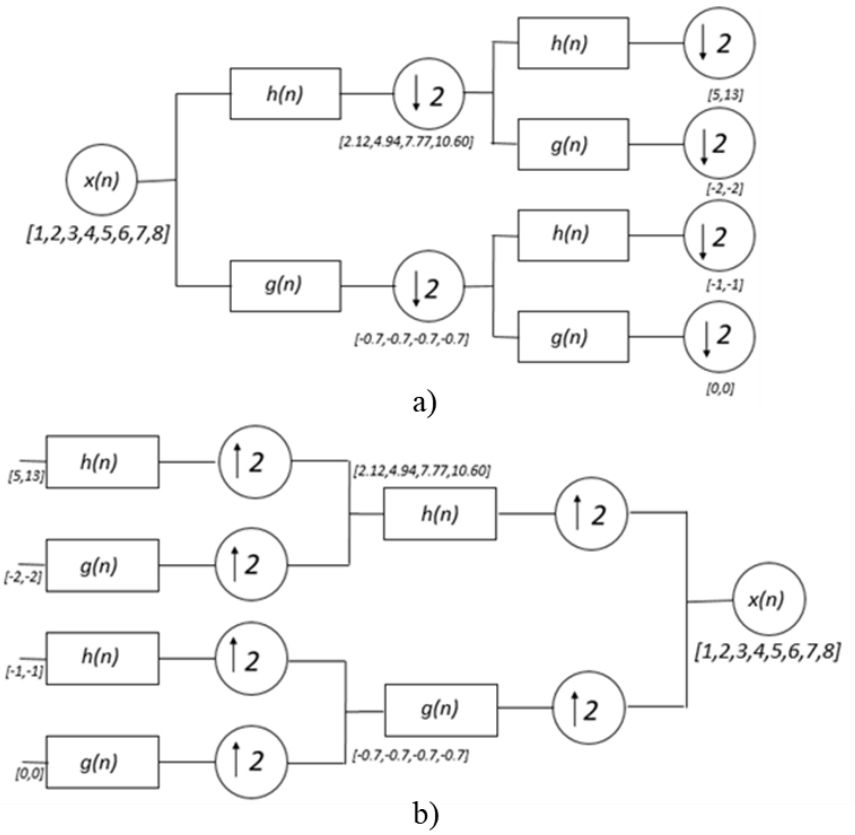

Fig. 2.8 Numerical WT using Mallat algorithm: a) transformed signal, b) recovered signal.

2.3.2 Compression Techniques

In general, the compression techniques are organized in two groups: the first one is the lossless compression [Sayood-00], which recovers the signal without losing information. The second one is the lossy compression [Sayood-00], which involves some loss of information. The wavelet function could take different waveforms, each of them called family. In this section, three different families are considered: Haar, Daubechies, and Coiflets.

WT compresses a signal using the lossy compression scheme; besides, WT is a useful technique to compress non-sparse and biomedical signals [Gandhi-11].

In the particular case of an EEG signal, compression using the Mallat algorithm can be achieved by eliminating the $g(n)$ transformed signal [Mallat-99]. This is possible because the information contained in high frequencies could be neglected. The recovered signal through

inverse WT tends to be similar to that one captured by the sensor. Note that the compressed signal lost a portion of the information and the system cannot recover the signal exactly as the original; this kind of compression is called lossy.

Give that WT is a lossy compression technique, it is important to measure the similarity between the recovered signal and the original signal. Literature presents different criteria to measure the signals, which are described in the next section.

2.3.3 Comparison Quantitative Criteria

In the literature, two different criteria to measure the similarity between the recovered signal and the original signal are considered: NMSE and PRD. CR is used to measure the ratio compression of the transformed signal. In this work, NMSE, PRD, and CR criteria are used to evaluate the performance of every wavelet family.

The first criterion is the NMSE [Zhang-13b], which measures the average of the square difference between the recovered and original signal. According to this criterion, when the result is closer to zero, the recovered signal is almost the exact original. The NMSE equation is given by

$$NMSE = \frac{\|x_k - \tilde{x}_k\|_2^2}{\|x_k\|_2^2} \tag{2-12}$$

where x_k is the original signal and $\tilde{x}_k$ is the recovered signal.

The second criterion is the PRD [Sriraam-08], which measures the difference between the recovered and the original signal. Here, if the result is around zero, then the recovered signal is close to the original. The PRD equation is given by

$$PRD = \sqrt{\frac{\sum_{k=1}^{N}(x_k - \tilde{x}_k)^2}{\sum_{k=1}^{N}(x_k)^2}}\ X\ 100 \tag{2-13}$$

Notice that a disadvantage of this criterion is present when the original signal has an offset, in which case the obtained values could be unreliable.

The third criterion is the CR [Zhang-13b], [Sriraam-08], which determines the compression rate percentage of the outcome. The corresponding equation is given by

$$CR = (1 - \frac{\widetilde{x_{k-length}}}{x_{k-length}})\ X\ 100 \tag{2-14}$$

where $x_{k\text{-}length}$ is the uncompressed signal length and $\tilde{x}_{k\text{-}length}$ is the compressed signal length. Finally, the performance of every algorithm is evaluated using NMSE, PRD and CR criteria. In

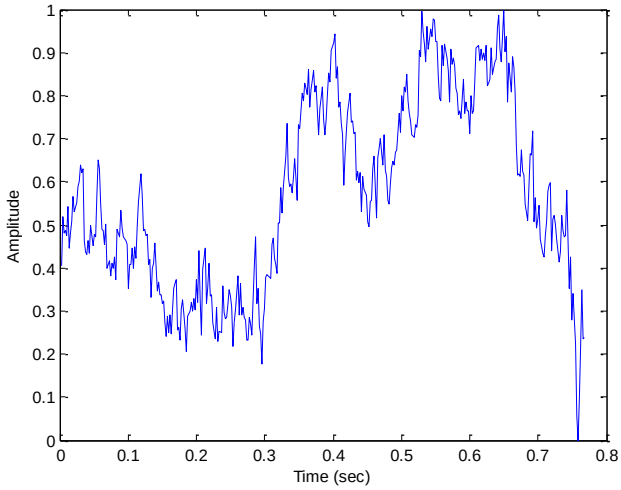

Fig. 2.9 EEG signal used for the experiments.

the next section, the simulations are described and results are presented.

2.4. EEG Compression Simulation and Results

The experiments are simulated in MatLab. The EEG signal data is obtained by [CODES-16], it has 386 samples, which represents 0.76 seconds from a healthy person. Fig. 2.9 shows the EEG signal used for the experimental part. The EEG signal is compressed using WT with three different families: Haar, Daubechies, and Coiflets; also, it is analyzed at different scales and finally it is recovered. Additionally, the BSBL algorithm [Gandhi-11] is used to compare our results. In order to determine the performance of every algorithm, NMSE, PRD, and CR criteria are considered. In order to compare algorithms in a fair manner, the experiments are conducted using the original signal for all algorithms and the amplitude of all signals are normalized.

According to (2-1), to scale WT it is necessary to change the value of j. The values of j used in the experiments are 2, 3, and 4.

Fig. 2.10 presents a comparison between the original EEG signal and the recovered signal using 3 different scales of the wavelet function and 3 different families: Haar, Daubechies, and Coiflets. It is seen that the best performance is obtained with the Haar family when $j = 2$.

Fig. 2.11 compares the results obtained with the Haar family with $j = 2$ against the BSBL algorithm. It shows that the results are similar. Quantitative results are presented in Table 2.1.

According to NMSE and PRD criteria, the best recovered signal is obtained by the Haar

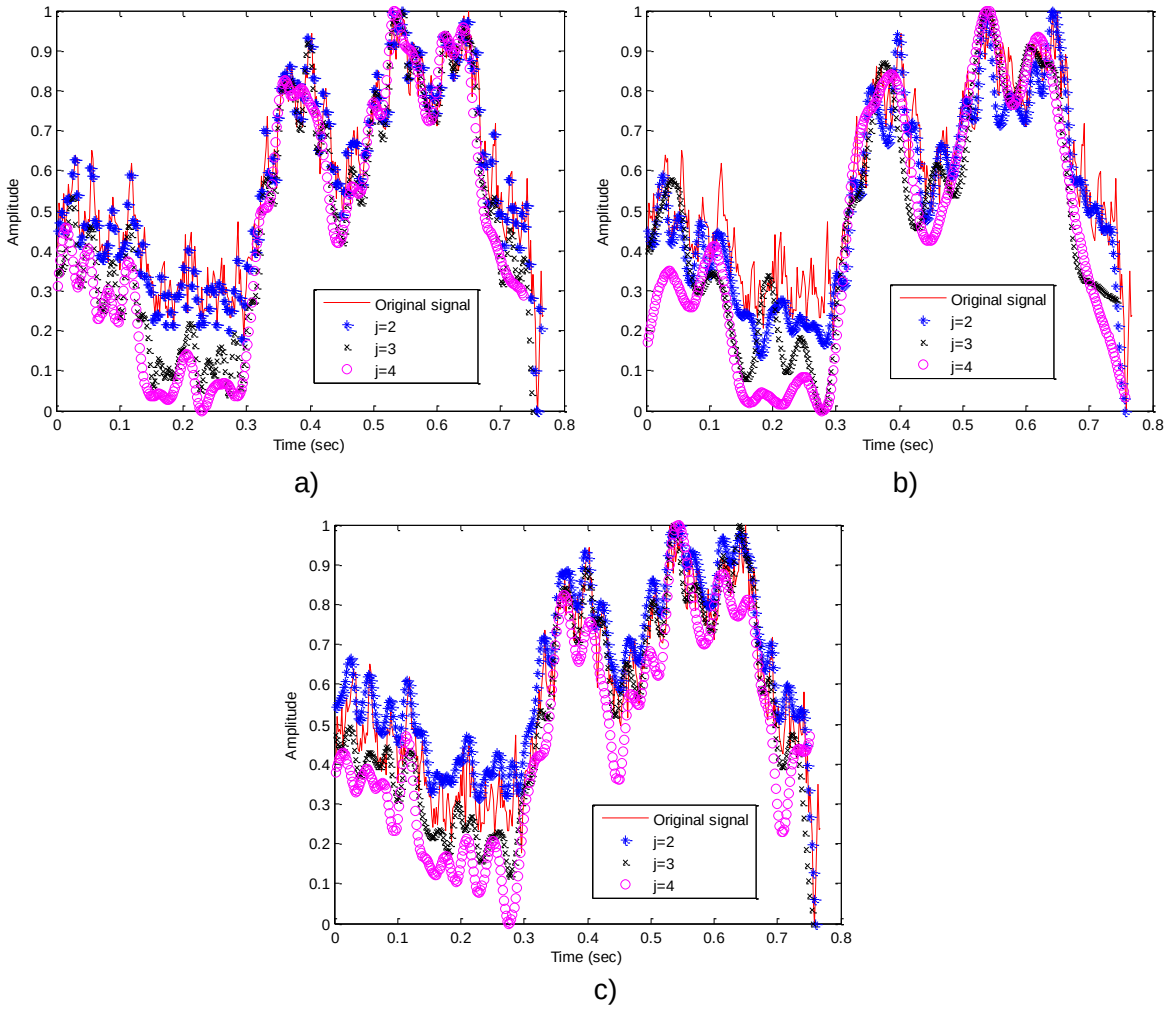

Fig. 2.10 Comparison between original and recovered signal using different scaled Wavelet families: a) Haar family, b) Daubechies family, c) Coiflets family.

family when $j = 2$. The Daubechies family presents the worst performance in all cases. The highest CR value is obtained by the Coiflets family when $j = 4$. Finally, the Haar family and the BSBL algorithm are compared and the best performance is obtained by the Haar family.

2.5. Conclusions

Different wavelet families were compared in this chapter in order to compress an EEG signal. The Coiflets family presented the best compression ratio (88% of the original signal) for the case $j = 4$, while the Haar family presents an adequate performance related to the NMSE and

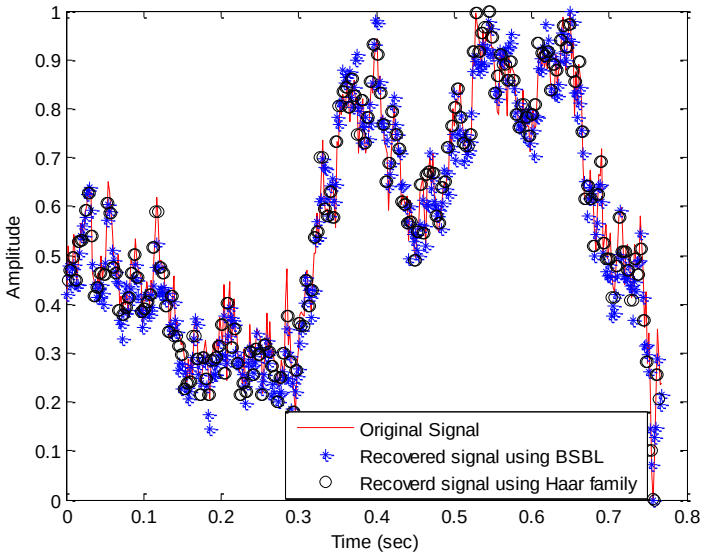

Fig. 2.11 Comparison between Haar family with the value of j = 2 and BSBL algorithm.

TABLE 2.1. COMPARISON BETWEEN ALGORITHMS USING DIFFERENT CRITERIA

Algorithm	j	NMSE	PRD	CR %
Haar	2	0.0264	6.30	50
Coiflets	2	0.1088	14.06	66.66
BSBL	-	0.0514	15.49	50
Haar	3	0.1813	20.98	75
Coiflets	3	0.3134	24.40	83.33
Daubechies	2	0.1636	25.47	50
Daubechies	3	0.2527	26.47	75
Haar	4	0.3136	26.96	87.7
Daubechies	4	0.3501	29.31	87.5
Coiflets	4	0.4021	30.67	88.87

PRD criteria.

The literature reports that the Coiflets family can be used to detect features of an EEG signal. However, the results presented in this chapter show that the Haar family has a better performance than the Coiflets family. Finally, for future work, predictors could be considered as another compression technique and the energy consumption of the system would be measured.

3. Epilepsy Seizure Detection Using an EEG Signal

Epilepsy is a chronic brain disorder that affects the patients' quality of life even when this disease is controlled. A real-time epilepsy detection warning requires constant monitoring of the EEG signal. Moreover, an EEG signal presents special features, such as heavy tail behavior and the distribution parameters that capture the epilepsy seizure. In this chapter, alpha-stable parameters are studied and a suggested alpha-stable estimator is compared to other estimators. Our results show that the alpha-stable parameters can be used to detect epilepsy seizures in real time with low computational complexity. Finally, the values of different parameters of the method are explored in order to reduce the processing time of the algorithm.

3.1. EEG Signal Modelling Based on Alpha-Stable Parameters

A signal probability density function is considered heavy tail when its tail decays slower than the exponential distribution tail. It represents a high variability signal with numerous spikes during the process [Manolakis-05]. Signals with heavy tail distribution can be located in a different environment, such as ocean engineering [Jian-05], meteorology science [Adler-98], or hydrology [Anderson-98]. On the other hand, an EEG signal is generated by the sum of millions of synchronous electrical potentials by neurons, where each electrical potential is considered identically and independently distributed (IID). The electrical potential in neurons produces spikes, causing the signal to have a heavy tail distribution [Bates-97]. According to the generalized central limit theorem, the sum of IID random variables shows a different and limited distribution. For that reason, the signal must be a member of the stable class [McCulloch-86].

The method to determine if a signal probability density function has a heavy tail is the Complementary Cumulative Density Function (CCDF). Fig. 3.1 shows the CCDF of an EEG signal versus the theoretical CCDF of three different distributions (Gaussian, exponential, and Pareto). The tail of the EEG signal shows a similar decay as the Pareto distribution, and thus validates that the EEG signal has a heavy tail.

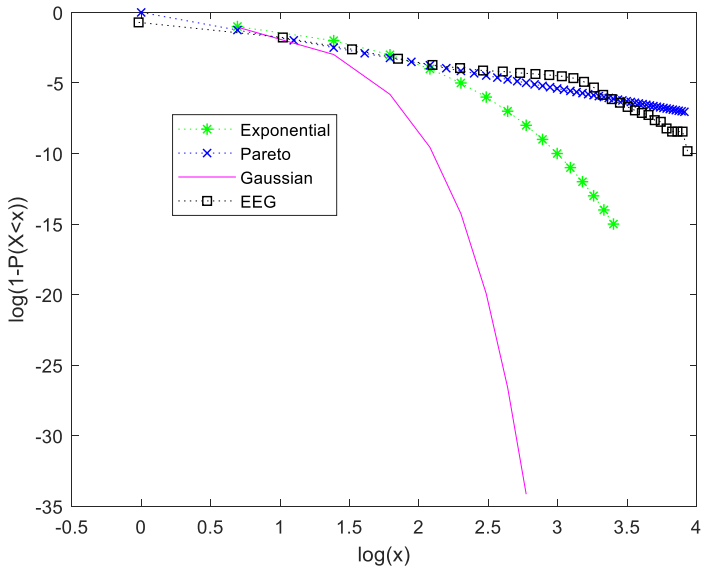

Fig. 3.1 Complementary Cumulative Density Function (CCDF) of the EEG signal.

For signals with a heavy tail, such as EEG, the calculation of alpha-stable parameters is a powerful computer technique to simulate features in a more realistic environment than the Gaussian case [Bates-97]. The alpha-stable parameters can be expressed using their characteristic equation given by [Samorodnitsky-94]:

$$Ee^{j\theta X} = \begin{cases} e^{\left\{-\delta^{\alpha}|\theta|^{\alpha}(1-j\beta(sign(\theta))\tan\frac{\pi\alpha}{2})+j\gamma\theta\right\}} & if\ \alpha \neq 1 \\ e^{\left\{-\delta|\theta|(1+j\beta\frac{2}{\pi}(sign(\theta))\ln|\theta|)+j\gamma\theta\right\}} & if\ \alpha = 1 \end{cases} \tag{3-1}$$

and

$$sign(\theta) = \begin{cases} 1 & for\ \theta > 0 \\ 0 & for\ \theta = 0 \\ -1 & for\ \theta < 0. \end{cases} \tag{3-2}$$

The full stable class of the equation is characterized by four parameters: the stability parameter, $\alpha \in (0,2]$; the symmetry parameter, $\beta \in [-1,1]$; the dispersion parameter, $\gamma \geq 0$; and the position parameter, $\delta \in \mathbb{R}$. Different features of the distribution can be obtained when α and β parameters change. For example: considering α, three different cases can occur: 1) when $S(x;2,\beta,\gamma,\delta)$ represents the Gaussian distribution, 2) $S(x;1,\beta,\gamma,\delta)$ represents the Cauchy distribution, and 3) $S(x;0.5,\beta,\gamma,\delta)$ represents the Levy distribution. On the other hand, when β changes, the symmetry of the distribution changes. When $S(x;\alpha,-1,\gamma,\delta)$ the distribution is skewed to the left, when $S(x;\alpha,0,\gamma,\delta)$ the distribution is symmetrical, and when $S(x;\alpha,1,\gamma,\delta)$

the distribution is skewed to the right [Bates-97]. The notation used for the class of stable laws are given by $S(x;\alpha,\beta,\gamma,\delta)$; where x is the independent signal [Samorodnitsky-94]. Nonetheless, a signal could have different characteristics that can be modeled if the alpha-stable parameters are changed. Given that the epileptic seizure modifies the hyperactivity of neurons affecting the alpha-stable parameters, we present in the next section an analysis of the impulsive EEG signal.

3.2. Epilepsy Detection

Alpha-stable parameters provide information about features of the signal. This information can be useful to detect diseases using the biomedical signal. The EEG signal has a reference since it has been demonstrated that when a patient has the Parkinson's syndrome, the distribution of the EEG signal tends to be Paretian [Salas-Gonzalez-14]. On the other hand, when a patient has an epileptic seizure the EEG signal changes and it can be compared with different distributions. For instance, Support Vector Machines (SVM) are used in [Wang-15] to compare the distribution of the EEG signal with a Gaussian and Cauchy distribution. Nevertheless, this process requires a high computational cost.

In order to facilitate the calculation of the alpha-stable parameters, different estimators have been designed [Anderson-98] and [Stevenson-07]. An estimator calculates the alpha-stable parameters as follows. First, the estimator calculates the Probability Density Function (PDF) of the signal. After that, every alpha-stable parameter is determined $S(x;\alpha,\beta,\gamma,\delta)$ [McCulloch-86]. In order to analyze the behavior of every parameter corresponding to an EEG signal, we compute the four alpha-stable parameters. In this work we use EEG signals obtained from the MIT database [MIT-14] which are 30-minutes long. The amplitude of the signal without seizures is 50 μV. The amplitude of the signal with seizures is 600 μV. Finally, the sampling frequency is 256 Hz. All the experiments are conducted using MATLAB. The procedure to obtain the parameters is as follows. Firstly, a window of the signal is obtained, and his CCDF and alpha-stable parameters are calculated using a window length of 0.36 seconds. After that, a consecutive window of the signal without overlap and the same length is taken, its parameters are calculated, and the process is repeated until the whole signal is analyzed. The outcome of the experiment is shown in Fig. 3.2.

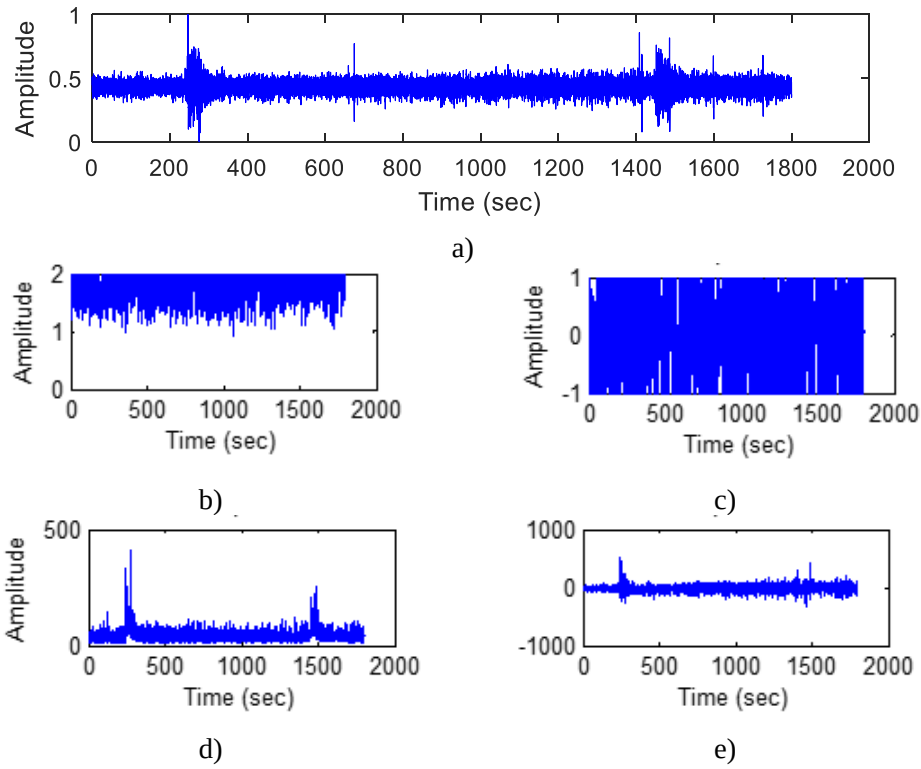

Fig. 3.2 Alpha-stable parameters: a) EEG signal, b) Alpha parameter, c) Beta parameter, d) Gamma parameter, e) Delta parameter.

The EEG signal with two epileptic seizures, in seconds 250 and 1450, is presented in Fig. 3.2a. The alpha-stable parameters alpha (Fig. 3.2b), beta (Fig. 3.2c), gamma (Fig. 3.2d), and delta (Fig. 3.2e) are shown. We can observe that beta and delta parameters are not sensitive to changes in the EEG signal. Alpha parameter, on the other hand, is greater than the value of 1.5, which shows that the EEG signal has a finite average. However, the alpha parameter does not provide relevant information to detect an epileptic seizure. Finally, the amplitude of the gamma parameter increases four or five times when an epileptic seizure occurs. Therefore, the gamma parameter can provide information to accurately detect an epileptic seizure.

Three of the most used algorithms to estimate alpha-stable parameters are McCulloch, Stablekull, and Nolan [Anderson-98], [MATLAB-16a], [MATLAB-16b] and [Stevenson-07]. Authors in [Bates-97] found that the McCulloch has the best performance when the value of the alpha parameter is larger than 1. However, it is important to evaluate the three algorithms to determine the best performance when the gamma parameter is analyzed.

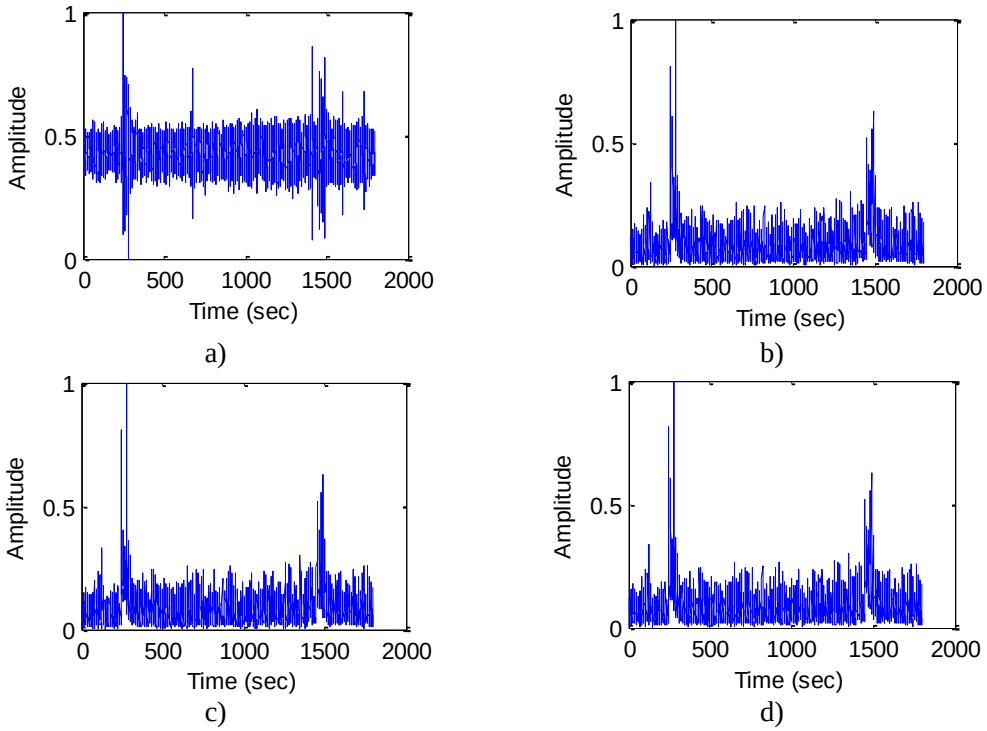

Fig. 3.3 Comparison of estimators, which calculate the gamma parameter: a) EEG signal with two seizures, b) Nolan algorithm, c) McCulloch algorithm, d) Stablekull algorithm.

TABLE 3.1. COMPARISON TIME BETWEEN ESTIMATORS

Estimator	Processing time (sec)
Nolan	684
McCulloch	953
Stablekull	1 350

A comparison between the estimator algorithms to calculate the gamma parameter is shown in Fig. 3.3: the EEG signal with two epileptic seizures (Fig. 3.3a), Nolan estimator algorithm (Fig. 3.3b), McCulloch estimator algorithm (Fig. 3.3c), and Stablekull estimator algorithm (Fig. 3.3d). In the three cases, the accuracy of the estimators is similar. Then, the processing time is evaluated and the result is shown in Table 3.1, where it is seen that the Nolan estimator, and not McCulloch's, is the fastest algorithm. Then, in order to evaluate the EEG signal, the Nolan estimator will be considered in future experiments.

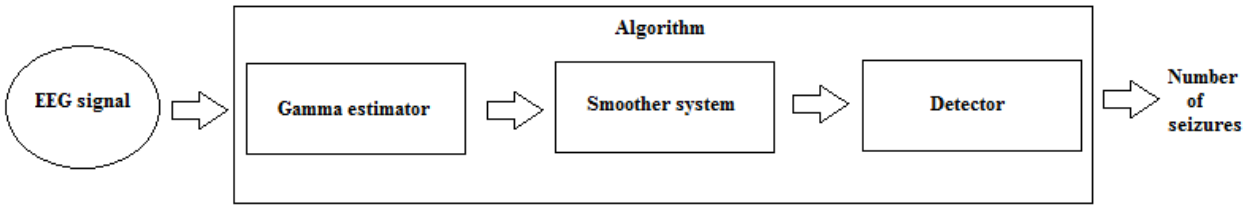

Fig. 3.4 Block diagram of the proposed algorithm to detect epileptic seizures.

3.3. Methodology

The algorithm described in this work is divided into three blocks: the gamma estimator block, the smoother system block, and the detector block. The block diagram of the complete system is presented in Fig. 3.4.

First, the system calculates the gamma parameter using the empiric CDF of the signal, for this the Nolan's estimator is used. Then, the gamma parameter is smoothed to reduce the influence of the noise. Finally, in order to detect epileptic attacks, the signal is analyzed using the detector block. A general description of each block is presented below.

3.3.1 Gamma Estimator Block

We choose the Nolan estimator to compute the gamma parameter. At the beginning of the process, the first w seconds of the EEG signal, a window of length w, are taken to perform the gamma calculation. A second length-w window is taken after n seconds from the first one and the gamma parameter is calculated. The process is repeated, shifting the window by n, until the whole EEG signal has been analyzed. In order to determine the best performance of the estimator, the length of the window is changed in subsequent iterations and the shifting of the window is the same as the length of the window.

3.3.2 Smoother System Block

In order to obtain a cleaner signal, the gamma parameter must be smoothed. Here, a

window of the gamma values signal is obtained. Then, the window is smoothed using an averaging filter. In the next step, the window is shifted *m* seconds, where $m \neq n$, and the process is repeated.

3.3.3 Detector Block

The last block of the algorithm is the detector, which considers two thresholds to avoid the false positive and true negative detections. The first threshold is the relation of the gamma samples values. The detector obtains two consecutive samples of the smoothed gamma. After that, both samples are compared. If the ratio between samples is larger than 5, then an epileptic seizure is detected. After that, the system waits for the amplitude of the gamma parameter to return to normal levels. If the amplitude of the gamma sample value does not return to the normal amplitude, then the system cannot detect more seizures. This part is considered as a second threshold.

3.4. Results

In this section, outcomes of every block of the system are presented. As stated before, the window length of the estimator and the smoother are changed in order to determine the best performance and reduce the processing time without losing accuracy. Finally, the complete system performance is discussed in the last part of the section. Through all the experiments, EEG signals from the MIT database [MIT-14] are used.

3.4.1 Gamma Estimator Block Results

Three different window lengths are considered to analyze the EEG signal: 0.03, 0.39, and 1.95 seconds. The shift time *n* used between windows is 0.03 seconds for all three cases. The outcomes of gamma estimation are shown in Fig. 3.5.

Fig. 3.5a shows the original EEG signal. Fig. 3.5b and Fig. 3.5c display the amplitude of the gamma parameter with an epileptic seizure, which is 7 times greater than the gamma parameter without an epileptic seizure. On the other hand, Fig. 3.5d shows that the amplitude of the gamma parameter is 5 times greater than the gamma parameter without an epileptic seizure. As a result, the window length estimate of the gamma parameter is not important because in all three cases,

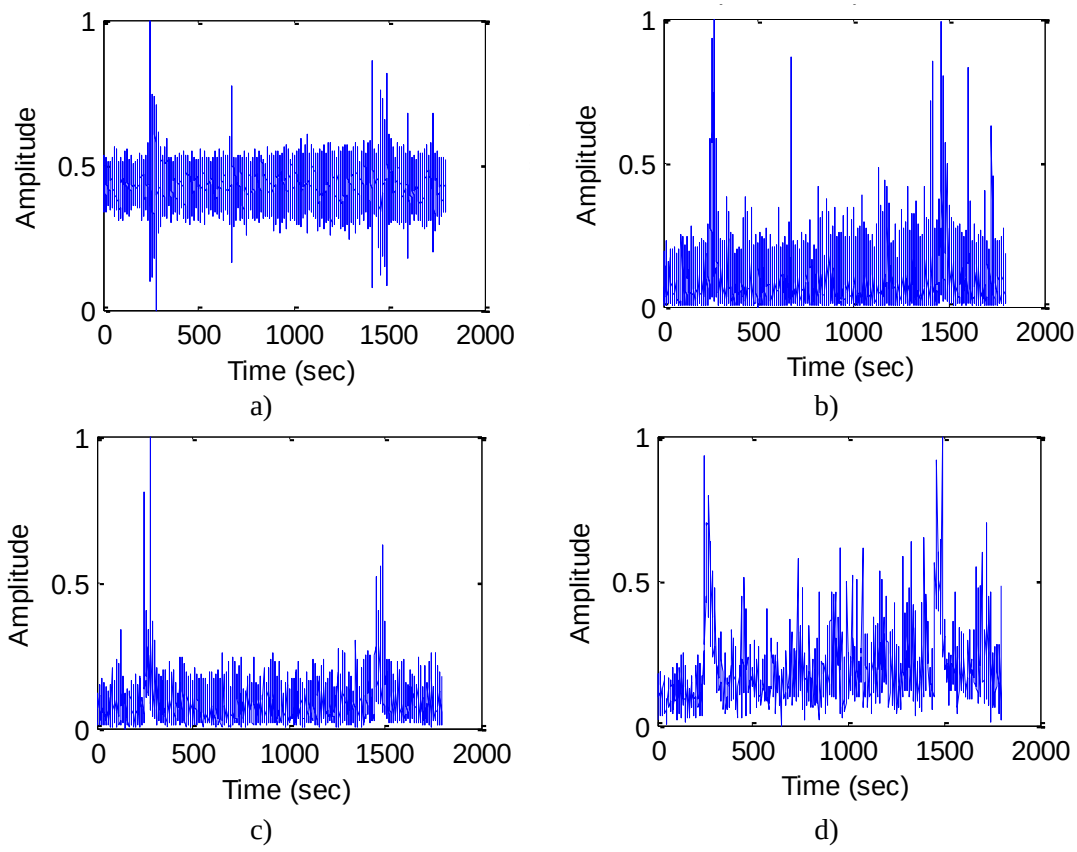

Fig. 3.5 Comparison of the gamma parameter estimation for different window-lengths: a) EEG signal, b) window length of 0.03 sec, c) window length of 0.39 sec, d) window length of 1.95 sec.

TABLE 3.2. COMPARISON OF THE PROCESSING TIME OF THE GAMMA ESTIMATOR BLOCK WITH DIFFERENT MOVING WINDOW LENGTH

Window length (Seconds)	Processing time (seconds)
0.03	2.8
0.39	0.31
1.95	0.16

the epileptic seizure is detected.

In order to obtain the performance of each window-length, the processing time is presented in Table 3.2. These results confirm that when the window is wider, the processing time is shorter. The best performance is obtained by the wider window with a length of 1.95 seconds.

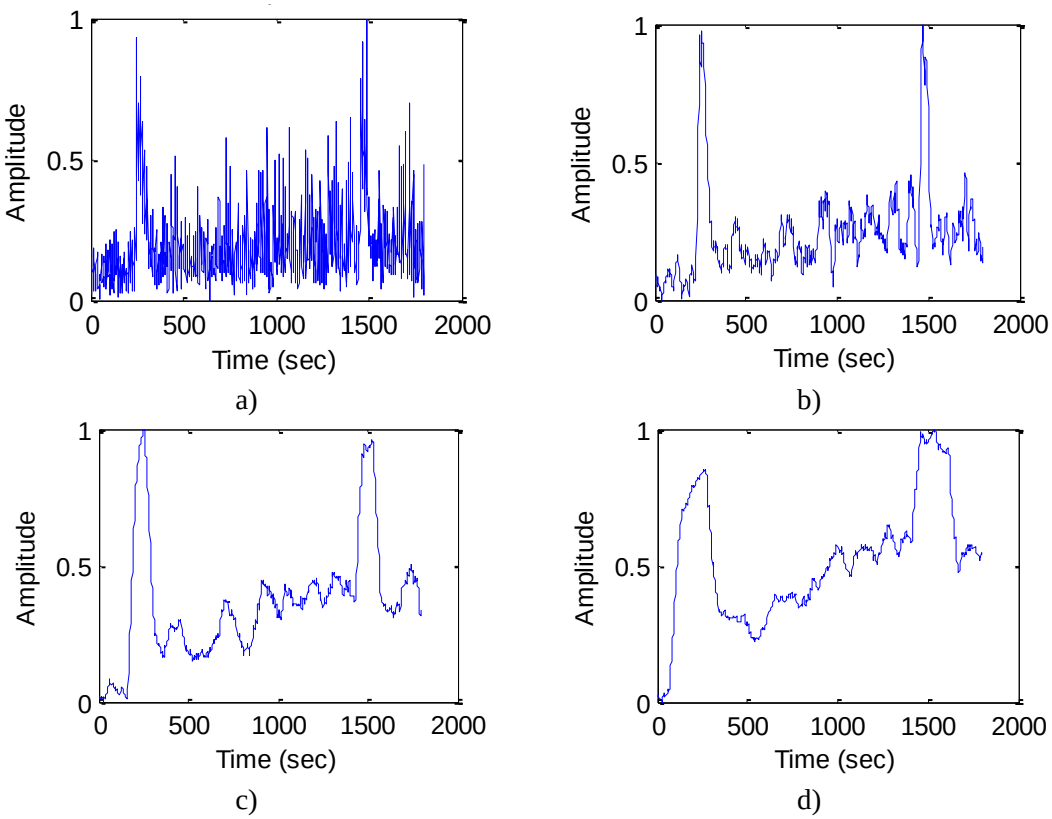

Fig. 3.6 Comparison of the smoother block outputs for different window-lengths: a) gamma parameter, b) window length of 0.03 sec, c) window length of 0.19 sec, d) window length of 0.39 sec.

3.4.2 Smoother System Block Results

After the gamma parameter is estimated, a smoothing filter is applied to reduce the influence of the noise. Here, again, a window of the gamma signal is defined. The length of it is changed in order to reduce the processing time of the block. Three different window lengths are considered (0.03, 0.19, and 0.39 seconds). The outcomes of the signal after the smoother block are presented in Fig. 3.6.

Fig. 3.6 shows that, if the window is wider, then the offset of the signal is larger. In all three cases, the epileptic seizure is detected. The processing time for each window-length is obtained using the "*tic-toc*" command of MATLAB and it is shown in Table 3.3; this is greater when the window length is longer. The best performance is obtained with the window length of 0.03 seconds.

TABLE 3.3. COMPARISON OF THE PROCESSING TIME OF THE SMOOTHER SYSTEM BLOCK WITH DIFFERENT MOVING WINDOW LENGTH

Window length (Seconds)	Processing time (seconds)
0.03	0.0089
0.19	0.0091
0.39	0.0096

3.4.3 Detector Block Results

The number of epileptic seizures are detected in this block. The outcomes of the experiments show that the system is accurate to detect epileptic seizures. On the other hand, the processing time to scan the smoothed gamma signal of 30 minutes is 0.0041 seconds. Finally, the overall processing time of the complete system is 0.1725 seconds.

3.5. Conclusions

A method to analyze an EEG signal and detect epileptic seizure using alpha-stable parameters was presented in this chapter. It was demonstrated that the EEG signal has a heavy tail distribution, and its tail tends to decay similarly to a Pareto distribution. When an epileptic seizure is present, the gamma parameter shows significant changes that can help to detect the disorder. The McCulloch, Stablekull, and Nolan estimators were evaluated for the computation of the alpha-stable parameters, resulting that Nolan is the one with the best performance.

An accurate algorithm to detect epileptic seizures is proposed. It can be shown that it is more sensitive than others reported in the literature and the processing time of the algorithm is shorter (the corresponding comparison is omitted for the sake of brevity). Variations in algorithm parameters showed that the best performance is obtained with a window-length of 1.95 seconds. Regarding the window-length in the smoother block, the best performance is obtained when the length is 0.03 seconds. Finally, the overall processing time required to analyze the complete EEG signal is 0.1725 seconds for a 30 minutes long EEG signal.

4. Breathing Signal and Sleep Apnea Detection Using UWB Technology

Sleep apnea is a syndrome that consists of a breathing pause of more than 10 seconds while a patient is sleeping. Diseases such as strokes, coronary heart attacks, or diabetes could be associated with an untreated sleep apnea. New methods to detect sleep apnea are based on the ultra-wide band UWB technology. UWB is a noninvasive, low power, and low radiation technique. In this chapter, the breathing signal of the patient is automatically detected from the variance of UWB signals reflected in a human body. This signal is analyzed and two sleep apnea detection methods are presented: the derivative and the cross-correlation of the breathing signal. It is demonstrated that our proposed algorithm detects accurately the breathing signal and sleep apnea in different patients.

4.1. Sleep Apnea

Sleep apnea is a syndrome which affects at least 6% of the adult population [WHO-17]. The sleep apnea is a breathing pause of 10 seconds or more while a person is sleeping. Occasionally, a normal person has apneas, however, a health damage is considered when the patient has at least 300 sleep apneas per night or its duration is around 5 minutes [AASM-17], [Guyton-11], and [Varady-03]. The sleep apnea is caused by the obstruction of the airways [Guyton-11] and it is divided into two types: central sleep apnea (CSA) and obstructive sleep apnea (OSA). In the CSA, the nervous central system does not send the impulse information to the airway muscles and they block the air conduct in the pharynx. On the other hand, the OSA is caused by soft tissues which block the airway conduct [Guyton-11] and [Varady-03]. In both cases, it could be accompanied by loud snoring [WHO-17]. After that, the snore is interrupted by a long silence. Finally, the brain sends an impulse to the patient to open the airway or move the body to continue breathing [Guyton-11]. A patient with sleep apnea could present different symptoms, such as feeling sleepy, sleeping during the day, being forgetful, having strong headaches, falling asleep while the patient is watching TV, working, driving, or reading, or waking up tired in the morning

[MEDLINE-17]. Other diseases associated with non-treated sleep apnea are: strokes, coronary heart disease, hypertension, or diabetes [NHLBI-17] and [Varady-03].

Currently, the most common medical method to diagnose sleep apnea is performed by the polysomnography [AASM-17] and [MEDLINE-17]. In this technique, an oxygen mask is placed on the nose and mouth of the patient while sleeping. Then, the device records the patient's breathing and it detects when the sleep apnea occurs, as well as its duration. There are others complementary tests that confirm sleep apnea, such as electrocardiography (ECG), echocardiography, thyroid test, or arterial blood test [MEDLINE-17]. Also, a non-invasive technique to detect sleep apnea is measured from the patient chest movements. For example, pressure transducers are placed on the patients' bed. When the patient inhales or exhales, the pressure exerted on the bed changes. When a sleep apnea occurs, the pressure of the body on the bed is steady for more than 10 seconds [Waters-09]. However, the patient must be in a specific position for the breathing frequency detection. Another technique is the Doppler radar, which measures the distance between the radar and the chest of the patient. If distances do not change for more than 10 seconds, then the sleep apnea alert is activated. Unfortunately, this technique in some cases tends to be inaccurate [Yue-11].

Recent experiments show that sleep apnea could be detected using the ultra-wide band (UWB) technology [Yue-11]. The approach in [Fedele-15] and [Yue-11] uses the UWB to measure the distance between the target and the device. On the other hand, in [Abib-14] they compare the distance measured using an UWB device versus the real distance. As a result, the chest displacement is estimated [Muller-15]. Nevertheless, the conclusion of this paper is that the maximum error range between the measured distance by the UWB device and the real distance is 3 cm in 25 cm. Therefore, that system shows some imprecisions. In [Karli-16] it is shown that the UWB signal changes with the human tissue.

According to the literature, UWB technology for detecting apnea has two principal advantages when measuring target's density instead of measuring distance. The first advantage is the accuracy of the device to detect the breathing signal of a patient, in contrast to measuring the distance, where chorea diseases such as Parkinson or Huntington could deteriorate the measurement accuracy [Fedele-15] and [Yue-11]. The second advantage is that even if the patient is under a thick blanket, density changes could be detected, unlike the measurement of distances, which may not detect the movement of the patient chest.

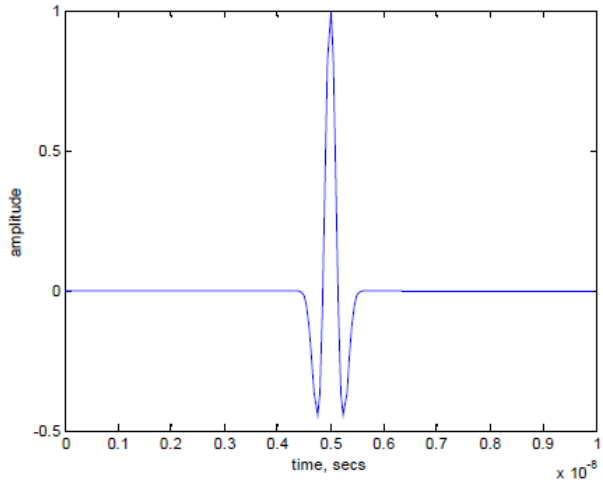

Fig. 4.1 Waveform of the Gaussian doublet pulse. Figure taken from [Pardiñas-Mir-09].

4.2. Ultra Wideband Technology

The Federal Communications Commission (FCC) of the United States of America (USA) defines the UWB technology as that one employing devices which transmit very short duration pulses that result in very large or wideband transmission bandwidths [Pardinas-Mir-09] and [Waters-09]. Typically, the largest pulse length considered as a UWB pulse is on the order of nanoseconds. The received energy signal is spread from close to DC to a few GHz [Pardinas-Mir-09].

The most common pulse used in the UWB technology is the Gaussian doublet, whose frequency spectrum nominal central frequency depends on the pulse width, as well as its spectrum bandwidth [Pardinas-Mir-12]. The Gaussian doublet pulse is shown in Fig. 4.1 and is given by:

$$g(t) = A\left[1 - 4\pi(\frac{t}{T_w})^2\right] e^{-2\pi(\frac{t}{T_w})^2} \quad (4\text{-}1)$$

where A is the maximum amplitude of the Gaussian doublet pulse, T_w is the pulse width, and t is time.

An advantage of this technology is that it has a low power spectral density, but with a very wide frequency spectrum. Thus, the UWB technology is robust in terms of security, because it is not easy to be detected or interfered by other technologies [Pardinas-Mir-09] and [Taylor-00]. Another advantage of this technology is that the multipath effects can be diminished, and it can penetrate through materials such as walls, doors, and windows [Pardinas-Mir-12].

a) b)

Fig. 4.2 UWB device: a) upper part, b) frontal part with antennas.

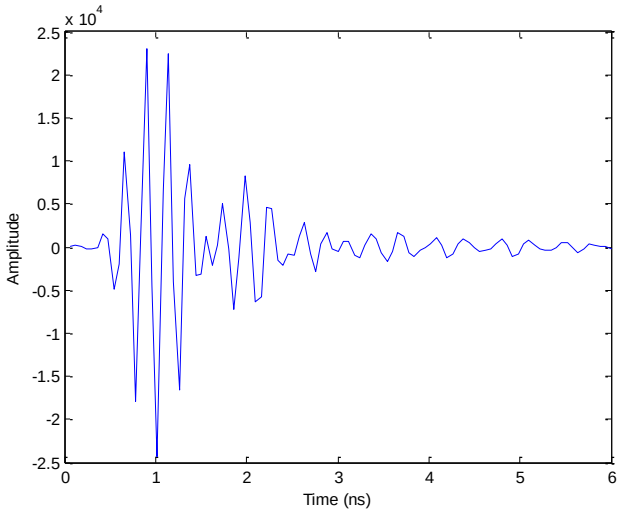

Fig. 4.3 The waveform of an UWB pulse produced by the transmitter.

UWB signals have been proposed for monitoring vital signs [Yue-11]. In this work, we use a UWB radar to acquire the breathing signal to which an algorithm to detect apnea is applied.

Fig. 4.2 shows the UWB radar device that was used in the experiments reported in this document. It is a monostatic radar module (MRM) model 410 from PulsOn that works in a frequency band between 3.1 and 4.8 GHz, transposing the UWB pulse to a center frequency of 4.3 GHz. This device has two antennas (Tx and Rx) in the same package. The UWB transmitter sends a pulse signal of 5.6 nano-seconds every 0.125 seconds to the target, which is shown in Fig. 4.3. Its bandwidth is presented in Fig. 4.4.

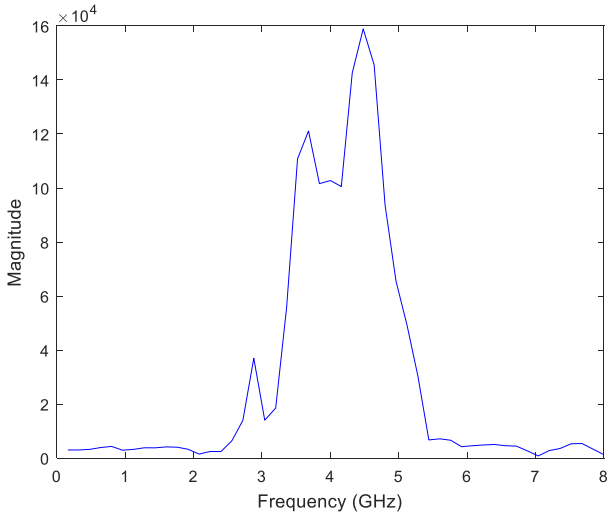

Fig. 4.4 The bandwidth of the UWB pulse presented in Fig. 4.3.

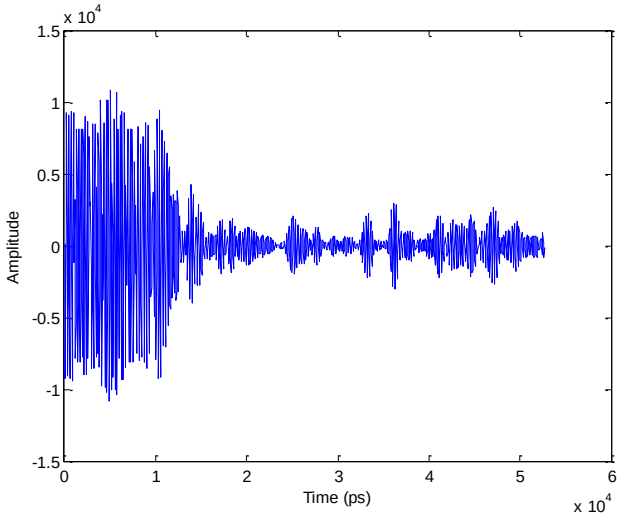

Fig. 4.5 Waveform of a realization collected from a range of 15.6 meters using the UWB device.

The transmitted signal is reflected on the target and arrives back to the receiver. The UWB receiver collects the reflected signal, samples it and stores it in an array of N received signals. Each sampled received signal is called realization. The work range of the device is around 15.6 meters. Depending of the configuration parameters, a typical realization (see Fig. 4.5) corresponds to 864 samples of 52 nanoseconds long received signal. The system can be configured for acquiring consecutive realizations for a given time period, for example, the time corresponding to several breathing cycles of a person.

The UWB device has the option of saving the collected realizations in cvs files, for subsequent processing by the user. The system also provides a MATLAB based software tool that can produce, from the collection of realizations, a signal representing the breathing of a person when the device is attempted to detect the chest movement of a person. In this case, the reflections of the rest of scenarios will produce scattering. The detection method proposed in this chapter takes as input the respiratory signal provided by the software.

4.3. Building the Breathing Signal

In [Servin-Aguilar-17], an overview of Ultra-Wide Band (UWB) signals and its use for obtaining a breathing signal is presented. In this section, we describe an aspect of UWB signals behavior in order to illustrate the way a breathing signal can be obtained from it when a UWB transceiver is targeted to a human body.

4.3.1 Behavior of UWB Signals

When a signal is transmitted in an ideal environment from point A to point B and is reflected back to point A in a direct path, without additional reflections, it is called the direct path. The total traveling time is known as time of flight TR. In a real environment, the signal that arrives to point B is composed of the direct path plus additional signals that are reflected in different objects (see Fig. 4.6), traveling longer paths and lasting for more than $TR/2$ seconds. Fig. 4.6 shows the way that the received signal, $d_{rT}(t)$, is constructed from different reflected signals or paths $d_{r1}(t)$, $d_{r2}(t)$, $d_{r3}(t)$, etc. In the case of a transceiver acting as a radar, the signals at point B are reflected and redirected to point A, where they are collected. This kind of UWB radar can be used to obtain a breathing signal of a person. The transceiver targets the person and sends one pulse, recording the received signal for T_L seconds, called a realization, ensuring that all paths have arrived. Doing this very fast and as many times, a signal representing the breathing can be obtained.

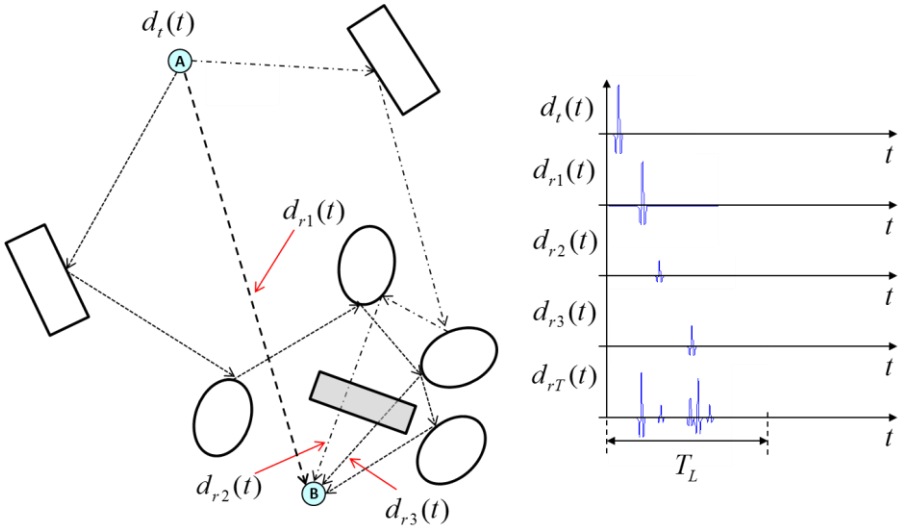

Fig. 4.6 Received signal constructed from reflections of the original signal on scatterers.

The time T_L is dependent on the longest distance to the object on which the signal is reflected. Hence, T_L corresponds to the time of flight of the longest signal path, so the maximal distance d_{max} that the transceiver can detect is half of that time:

$$d_{max} = \frac{T_L}{2} V_p \tag{4-2}$$

where V_p is the velocity of propagation. For example, a typical value of T_L for the transceiver used during the experiments presented in this document is 54 ns, then the maximum distance at which a target can be from the transmitter for being recorded is around 8 meters.

As stated before, in order to detect the cycle of the breathing signal of a person, it is necessary to analyze the signals corresponding to several cycles of breathing, which means a set of many realizations. The aim is to identify, in those signals, the information associated with the *x* axis value to the time position that indicates where is the target positioned. In order to standardize the identification concept, this method will be called the target position. The analysis of the target position is made through all realizations. The normal breathing frequency of a patient is approximately 12 times per minute, that means that the patient inhales and exhales every 5 seconds. However, the breathing frequency could change according to the patient and his status, where the minimum breathing frequency to live for a short time is 2 times per minute and the maximum is 40 times per minute [Guyton-11]. According to the sampling theorem, the minimum sampling frequency must be at least more than twice the frequency of the signal. In this case, the breathing

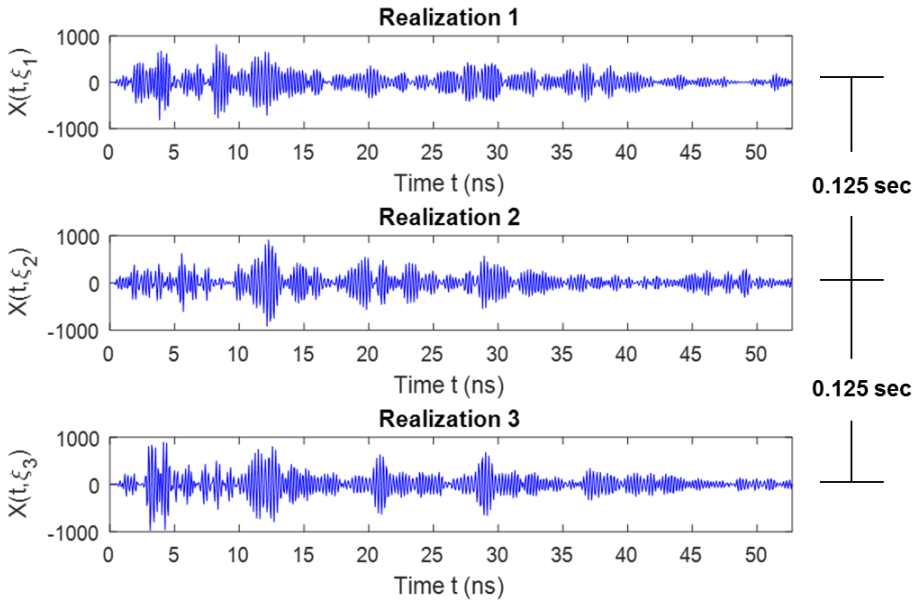

Fig. 4.7 Three realizations from a set of signals from the UWB system.

frequency is 0.2 Hz and the sampling frequency is normally set to 8 Hz, which is the transmission frequency of the set of pulses produced by the UWB system. One set usually consists of 20 realizations in order to detect one respiratory cycle of around 5 seconds. Fig. 4.7 illustrates three realizations from a set, where the time between them is 0.125 s.

4.3.2 Manual Distance Calculation and the Breathing Signal

One way to identify the time position of the target through a realization, is knowing in advance the distance at which the object is from the UWB transceiver. Then, the time position is easily calculated using:

$$t = {}^{d}/_{V_p} \tag{4-3}$$

where V_p is the propagation velocity ($3x10^8\ {}^{m}/_{s}$), d is double the distance between the target and the UWB device, and *t* is the propagation wave time (round trip).

For example, if the patient is at 70 cm from the UWB device, then the arriving time is 4.6 ns. Note that it is important to consider that the distance must be considered as twice the distance between the UWB device and the patient, since the signal travels that distance twice. After the

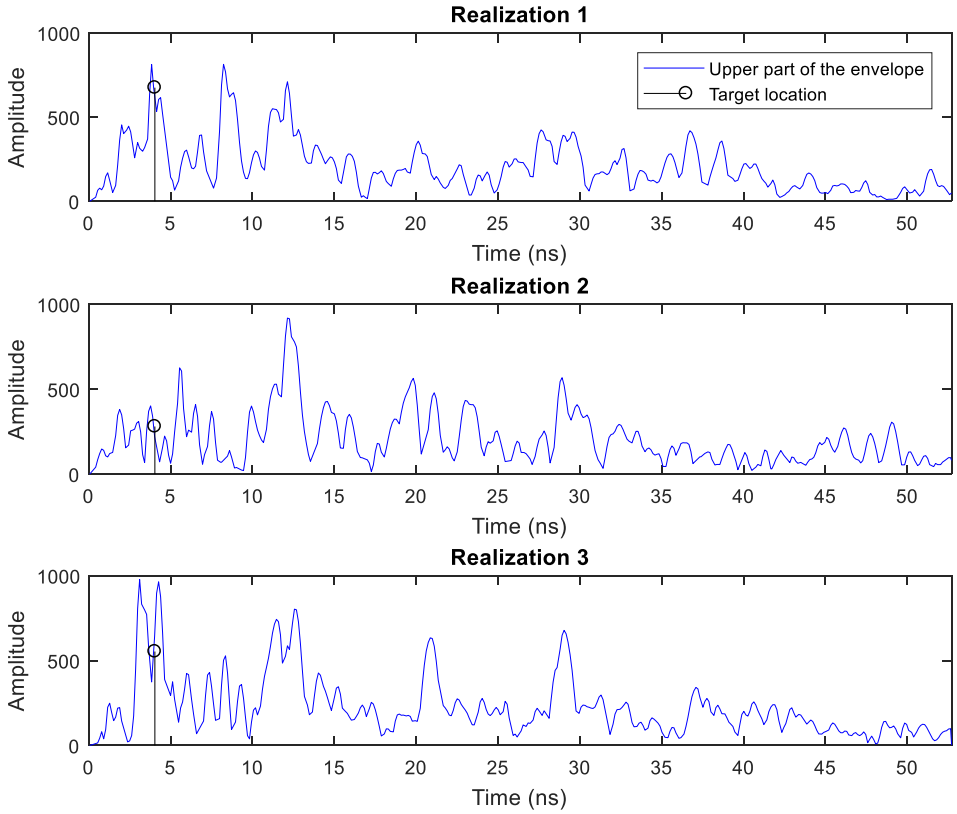

Fig. 4.8 Identifying the time position in the envelope through realizations using the velocity equation method.

position of the patient is located through the realization, the absolute amplitude value at the same point in all of the realizations set is analyzed, forming a signal. This signal corresponds to the amplitude variations of reflected signals at the target located at the corresponding distance. Knowing that the target is in fact a breathing human, then the amplitude of signals reflected at his chest will change according to the chest movement and the density change of the inner body at this point. In order to obtain the true amplitude value, the amplitude of the envelope signal is analyzed. Fig. 4.8 shows the amplitude envelope of three consecutive realizations, where the time point of the body position is located.

The amplitude values at these points are samples of the breathing signal that are built from analyzing all the realizations of the set, which is illustrated in Fig. 4.9. For instance, if the realizations are produced each 0.125 s, then this is the time separation between samples in the breathing signal.

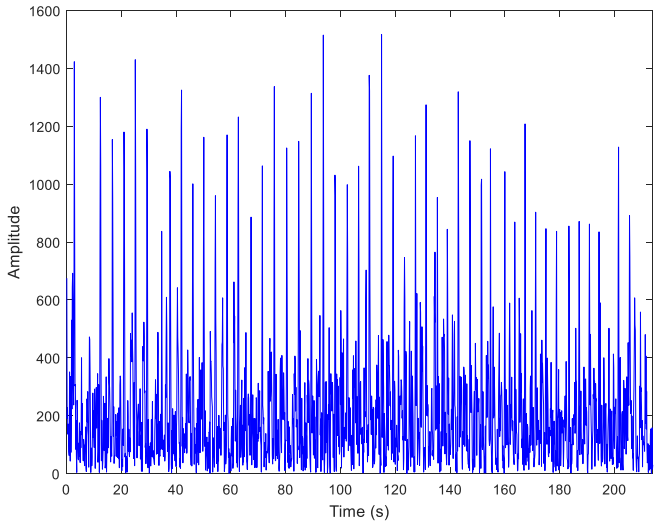

Fig. 4.9 Breathing signal of the patient from the manual calculation of its time position in a realization.

4.3.3 Automatically Obtaining the Breathing Signal

In order to calculate automatically the time position into a realization, and from this position to obtain the breathing signal, a method based on the signal variance is applied. In this method, the variance of the amplitude values at the same time position through all realizations is calculated by using:

$$VAR\{x\} = \int_{-\infty}^{\infty} (x - \mathrm{E}\{x\})^2 f_{x(t)}(x) dx \tag{4-4}$$

where x is the random variable (r.v.) of the process $X(t)$ for the realization ξ_n, $E\{x\}$ is the expected value of mean of the r.v., and $f_{x(t)}(x)$ is the probability density function (PDF) of $X(t)$.

The variance provides a measure of the amplitude dispersion with respect to the mean amplitude of the signal at time t. Then, the higher values correspond to the positions where the object made the signal amplitude change, as is the case with a static person breathing. An example of the variance of realizations is presented in Fig. 4.10, where two objects that vary the amplitude of the signal are clearly recognized. The maximum amplitude of the variance is obtained at 4.3 ns. In other words, the arriving time of the signal, which is reflected on the patient, is equal to 4.3 ns. A second object could produce the second peak or it could be the reflection of the first recognized signal. Once the time position is known, at 4.3 ns, the amplitude envelopes of all realizations are analyzed at this time position as in the manual calculation case, in order to obtain the breathing

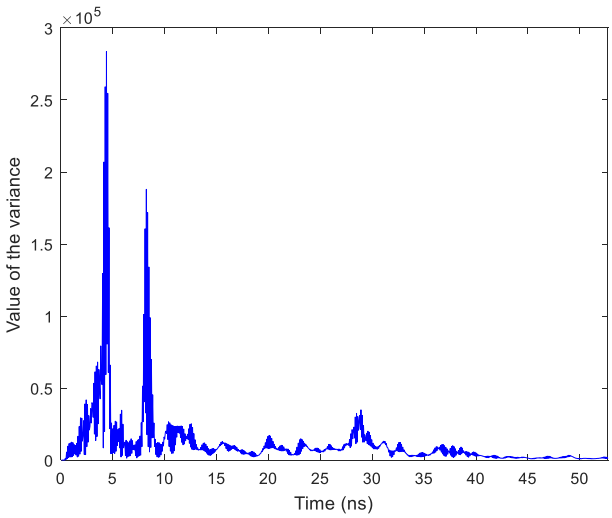

Fig. 4.10 The variance of realizations.

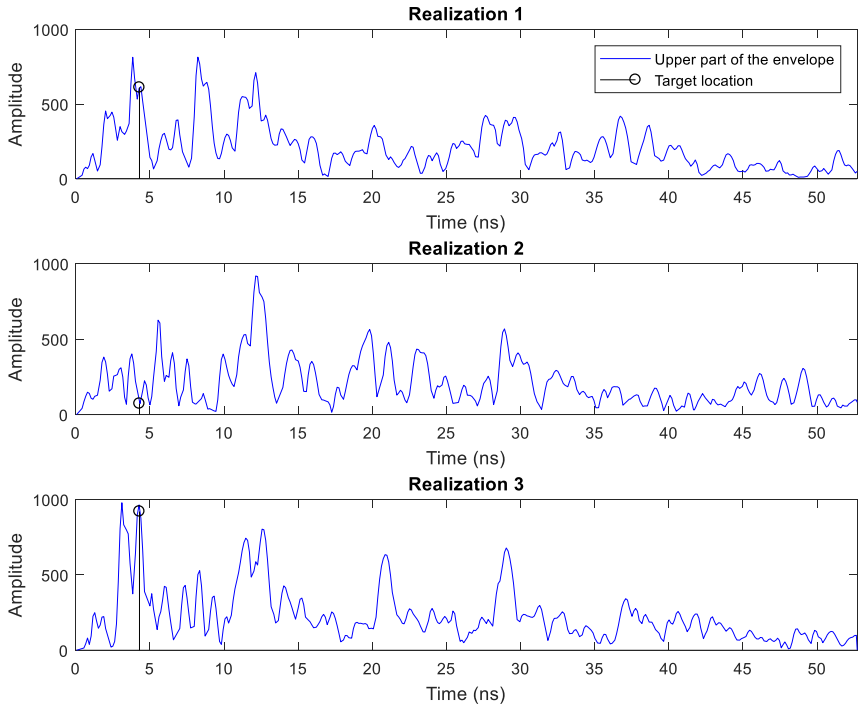

Fig. 4.11 Identifying the time position in the envelope through realizations using the variance method.

signal.

Fig. 4.11 shows the amplitude envelopes of three consecutive realizations, showing the time position where the target was found. The whole breathing signal obtained by the automatic calculation of time position is shown in Fig. 4.12.

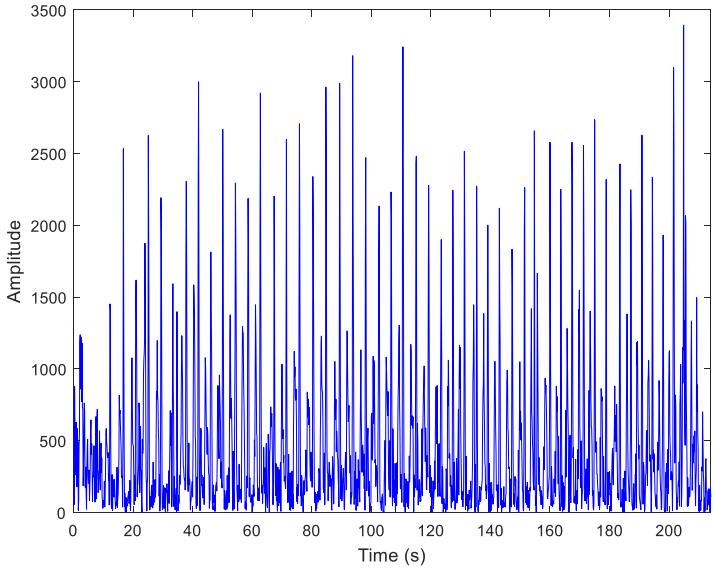

Fig. 4.12 Breathing signal of the patient using the variance.

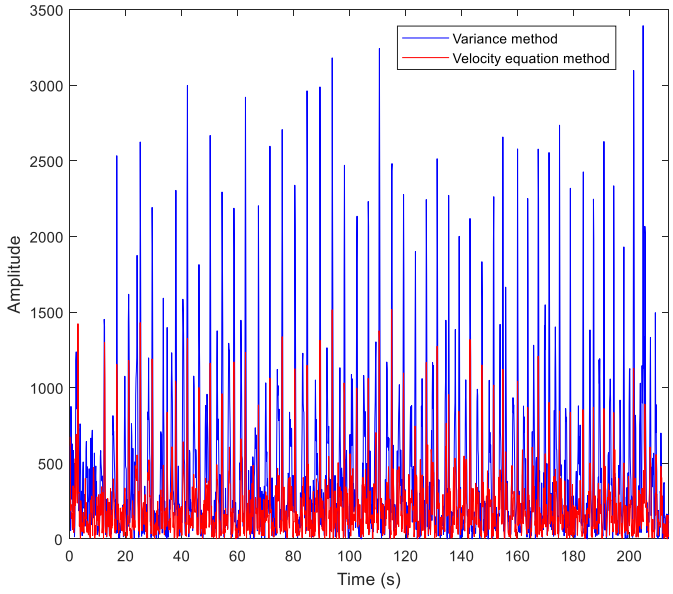

Fig. 4.13 Comparison of the breathing signal acquisition of a patient using velocity and variance methods.

Fig. 4.13 shows simultaneously the breathing signal obtained by the two methods: manual and automatic. We can see that both methods produce a similar signal. In the next section, we show the results of a series of experiments conducted to validate the automatic recognition of the

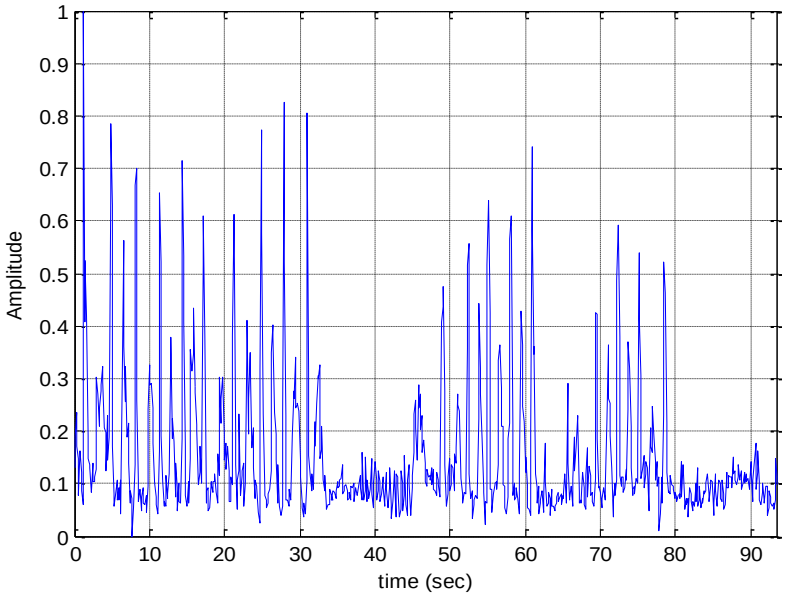

Fig. 4.14 Breathing signal with two sleep apneas starting at seconds 33 and 80.

target.

4.4. Proposed Algorithm to Detect Sleep Apnea

Once the breathing signal is acquired, the next step is to detect the sleep apnea. Fig. 4.14 shows a breathing signal with a sleep apnea, which is noisy. Here, we can identify two sleep apneas starting at seconds 33 and 80. If the signal is too noisy, the apnea could not be detected by the system.

In this section, two methods are considered for a reliable detection of the apnea: the derivate of the breathing signal and the use of correlation.

The first method detects apnea through the derivate of the breathing signal, which tends to detect abrupt changes in the signal. In this case, when the patient stops breathing, the changes produced by the chest cease, so the calculation of the derivative results in values close to zero. The criterion to decide if the patient is into an apnea state is for the derivative resting close to a value of zero for more than 10 seconds. The derivative equation is given by:

$$y(t) = \frac{dx(t)}{dt} \tag{4-5}$$

The second method is the correlation. In this method, a portion of the signal equivalent to a respiratory cycle (inhale and exhale once) is considered. This signal piece, called a breathing

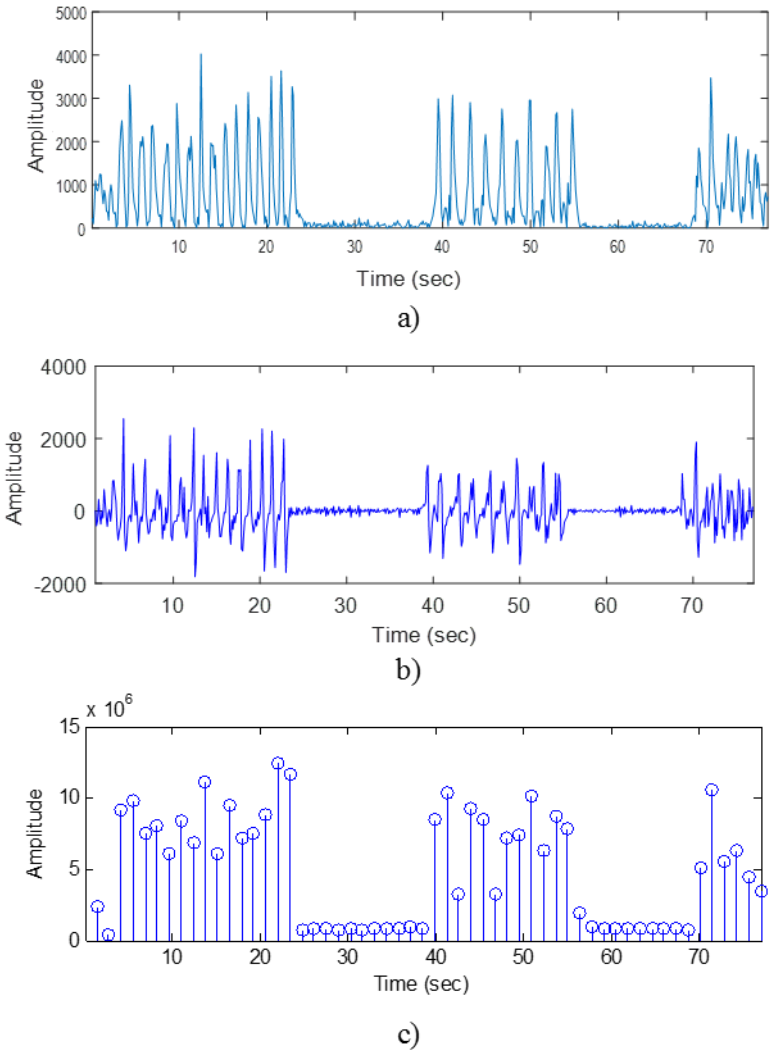

Fig. 4.15 Breathing signal, derivative, and correlation: a) breathing signal of a patient with two apneas at 24 and 55 seconds, b) derivative of the breathing signal, c) correlation coefficients calculated by the proposed algorithm.

frame, is correlated with the complete breathing signal.

When sleep apnea occurs $r_{x,y}(\tau)$ is approximated to zero for more than 10 seconds. The mathematical expression is given by:

$$r_{x,y}(\tau) = \int_{-\infty}^{\infty} x(t)y(t-\tau)dt \tag{4-6}$$

where $x(t)$ is the complete breathing signal and $y(t-\tau)$ is the breathing frame.

Fig. 4.15 shows 3 signals, in order to clarify the sleep apnea in a patient using the derivative and the correlation method in his breathing signal. Fig. 4.15a shows the breathing signal of the patient. Fig. 4.15b presents the derivative method. Fig. 4.15c depicts the correlation method.

4.5. Basic Sleep Apnea Detection Method Experimental Evaluation

The automatic method to obtain the breathing signal is validated trough some experiments carried out at two different environments: an electronics laboratory and a dormitory.

4.5.1 Experiments Description

The first series of experiments is performed in a laboratory. The UWB transceiver is targeted to the chest of the patient and the data are logged. In a first experiment, the patient is placed in front of the UWB device, which is moved from 20 cm to 100 cm. The objective of this experiment is to determine the maximum distance that the UWB could detect the movement of the patient's chest. In a second experiment, different patients are placed in front of the UWB at 60 cm. The aim of this experiment is to obtain the breathing signal of different people.

The second series of experiments are conducted in a dormitory, with the aim of obtaining data in more realistic conditions. The UWB device is placed at 60 cm of the bed and targeted to the chest of the patient. In a first experiment, the patient is lying on his side. First, the patient uses only a shirt, and after that, a blanket is placed over the patient. This experiment is conducted in order to determine if the breathing signal can be obtained in a real environment in different circumstances. In a second experiment, data of two different patients under the same conditions are obtained.

4.5.2 Experiments Results

In the first series of experiments, the maximum distances between the target and the UWB device to detect the breathing signal are obtained. The UWB device is aimed to the patient chest and it is located at 20 cm, 60 cm, 80 cm and 100 cm from the patient.

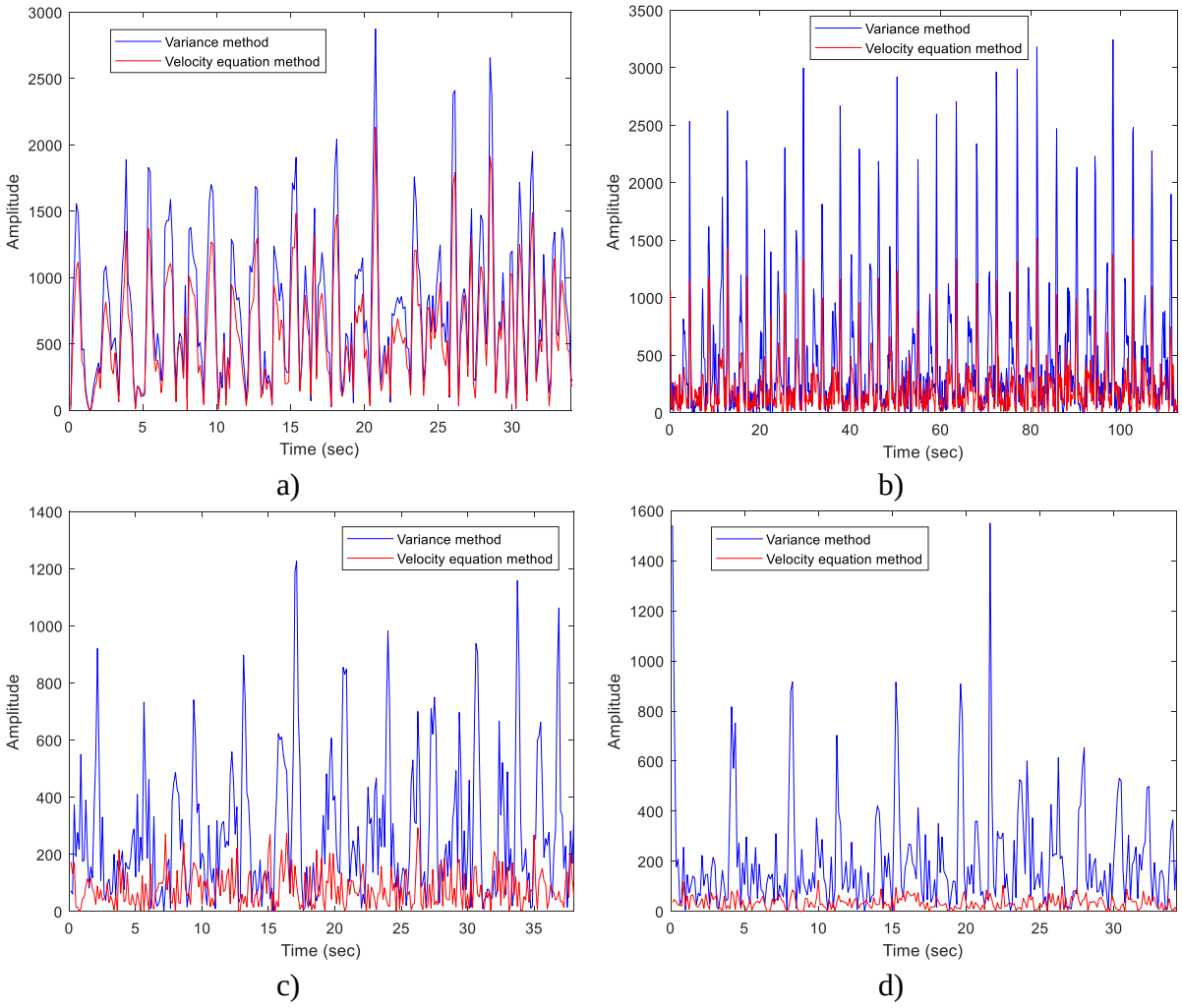

Fig. 4.16 Breathing signal of the patient at different distances: a) 20 cm, b) 60 cm, c) 80 cm, and d) 100 cm.

TABLE 4.1. PROCESSING TIME TO OBTAIN THE BREATHING SIGNAL RELATED TO THE DISTANCE

Distance (cm)	Manual method (sec)	Variance method (sec)
20	0.052	0.064
60	0.914	0.983
80	0.035	0.047
100	0.032	0.043

Some results are shown in Fig. 4.16, including the manual method of finding the target time position and the automatic one through the variance. The distances considered are: 20 cm (Fig. 4.16a), 60 cm (Fig. 4.16b), 80 cm (Fig. 4.16c), and 100 cm (Fig. 4.16d). In all of these cases,

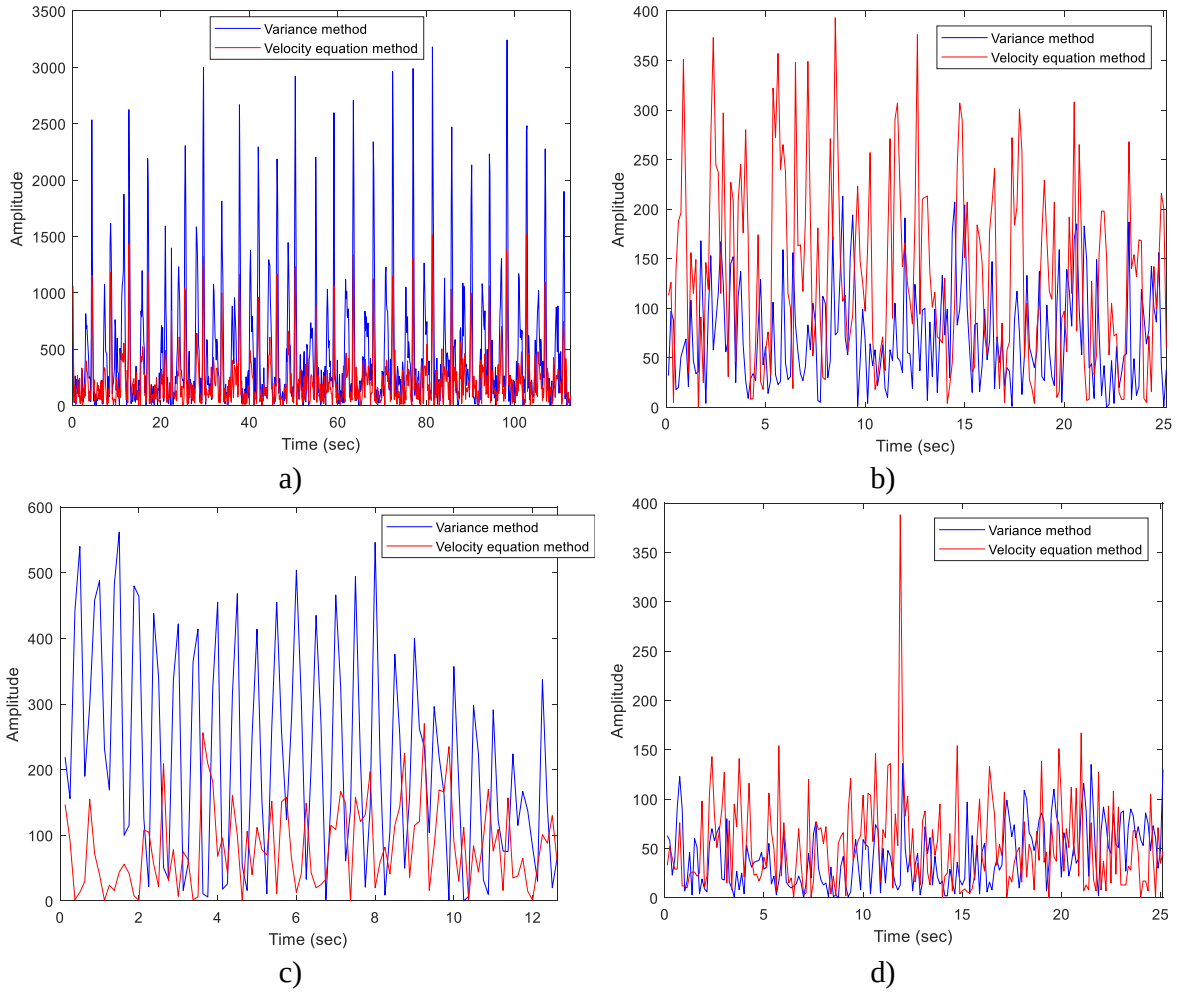

Fig. 4.17 Breathing signal of four different patients: a) Male I, b) Female I, c) Male II, and d) Female II.

the amplitude of the signal using the variance method is larger than that one using the manual computation of time position; additionally, for distances larger than 60 cm the amplitude of the latter is completely reduced. This indicates that the automatic method founds a better time position than the velocity equation computation. In order to evaluate the performance of both methods in terms of computing time,

Table 4.1 presents the processing time for each method. The reference is the manual computation of target's time position, in the 2nd column, while the 3rd column shows the processing time of the variance method. As mentioned before, the latter achieves the maximum distance between the UWB device and the patient, guarantying a good breathing signal at 100 cm.

In the next test, four people are considered to obtain their breathing signal. In all cases, the

TABLE 4.2. PROCESSING TIME TO OBTAIN THE BREATHING SIGNAL RELATED TO DIFFERENT PATIENTS (DIFFERENT BREATHING FREQUENCY)

Patient	Manual method (sec)	Variance method (sec)
Female I	0.049	0.064
Female II	0.047	0.076
Male I	0.914	0.983
Male II	0.056	0.067

distance between the UWB device and the target is 60 cm. Fig. 4.17 shows the breathing signal of these 4 different patients: two males and two females, with ages between 28 and 50 years.

Each patient has a different breathing frequency and yields a different received signal power. For example, in the breathing signal of male I and female II, the amplitude of the signal is larger using the variance method. On another hand, in the breathing signal of male II and female I, the amplitude of the signal is higher using the velocity equation method. However, in the case of male II and female II, the breathing signal is not clearly detected using the velocity equation method. In order to complete the experiment, the processing time is calculated and shown in Table 4.2. The difference in processing time is very small between both methods.

The second series of experiments, performed in the dormitory, are conducted under two different scenarios. In the first scenario, the patient is wearing a shirt. In the second scenario, a blanket is placed over the patient. The objective of this experiment is to determine if the UWB device can detect the breathing signal in more realistic environments. Results are shown in Fig. 4.18.

The breathing signal of the patient when he is wearing a shirt is shown in Fig. 4.18a, while that one when he has a blanket over him is presented in Fig. 4.18b. It is seen that the amplitude of the breathing signal is lower when the patient has a blanket over him, as expected. It is also seen that both methods detect the breathing signal in both scenarios. The corresponding processing time for both methods is presented in Table 4.4, where it is confirmed again a very small difference.

In the last experiment of the second series, two patients are considered: a 2-year old female and a 32-year old male. The male in this experiment is the same as male II in the laboratory environment series of experiments. The results are presented in Fig. 4.19: the breathing signal of the female III is in Fig. 4.19a, while that for male II is in Fig. 4.19b. It is seen a good performance of the variance method to obtain the breathing signal. The corresponding processing times are

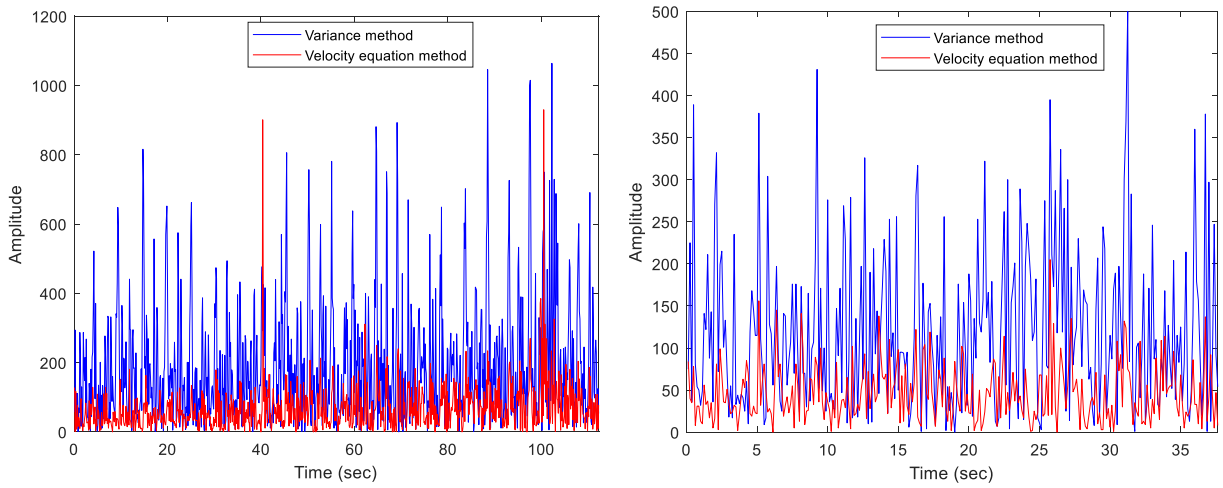

Fig. 4.18 Breathing signal of a patient on a bed: a) wearing a shirt, b) with a blanket over him.

TABLE 4.3. PROCESSING TIME USED FOR METHODS TO OBTAIN THE BREATHING SIGNAL CONSIDERING TWO DIFFERENT PATIENTS

Patient	Velocity equation method (sec)	Variance method (sec)
Female III	0.289	0.32
Male II	0.232	0.243

given in Table 4.3.

4.6. Conclusions

An automatic method to detect the breathing signal based on its variance was designed and proved to be effective considering different patients and environments. The proposed variance method showed a good performance in terms of distance and processing time. It was found that the proposed system presented the following restriction: beyond 100 cm, the breathing signal was not measured with sufficient accuracy. However, within a 100-cm range, both the sleep apnea and the breathing frequency were detected efficiently.

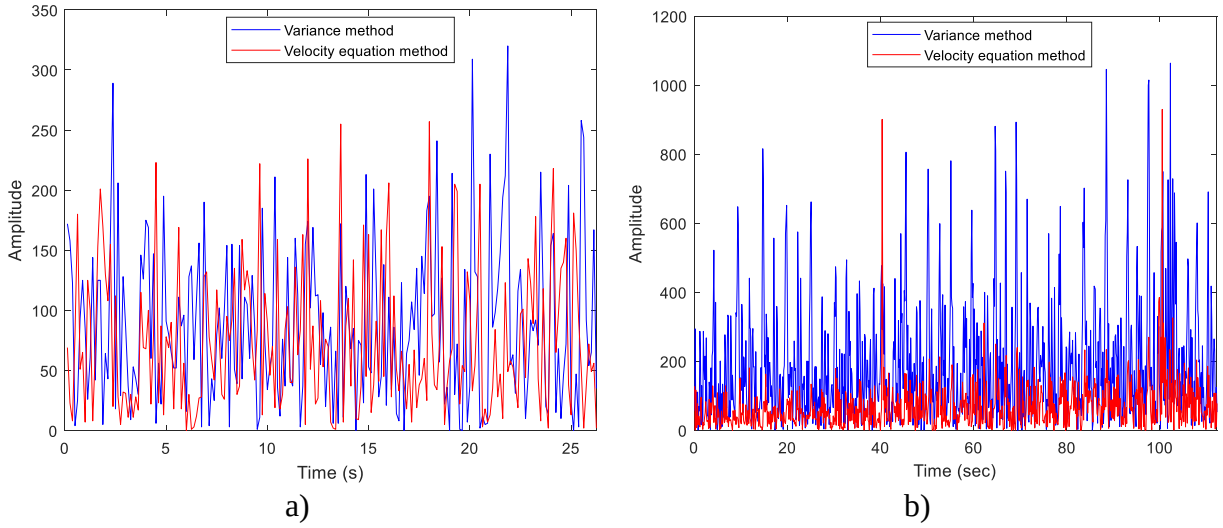

Fig. 4.19 Breathing signal of different patients on a bed: a) female III, b) male II.

TABLE 4.4. PROCESSING TIME TO OBTAIN THE BREATHING SIGNAL CONSIDERING TWO DIFFERENT SCENARIOS

Scenario	Manual method (sec)	Variance method (sec)
Wearing a shirt	0.232	0.243
Blanket over the patient	0.219	0.232

5. A New Method to Detect Sleep Apnea Using UWB Technology

UWB technology can be applied to obtain a breathing signal of a person and detect the sleep apnea disorder. This chapter presents a sleep apnea detection method based on a UWB radar targeting the sleeping person. The method is based on measuring the variance of the breathing signal continuously, identifying the changes that occur when the person has pauses in their breathing. Additionally, many experiments have been made in order to obtain the best values of three parameters that define the method based on variance. The criteria applied was the lowest processing load with the highest correct results.

5.1. Methodology

The method presented in this chapter is based on a UWB transceiver acquiring the reflected signals from a human body, as explained in the previous chapter. Instead of trying to identify the breathing cycle, the received signals (realizations) are processed to detect signal variations corresponding to a change of breathing. This is made by computing its variance and comparing the values from one realization to the next one, no matter at what point in the signal this variation occurs. While a person is breathing, the variance of realizations does not change suddenly, but when the person stops breathing the variance has a big change, signaling that apnea has occurred if it lasts for more than 10 seconds. Note that the breathing frequency of a patient is around 0.2 Hz or a breathing period of 5 seconds. The flowchart of this method is shown in Fig. 5.1.

The variance of a signal, as used in this work, provides a measure of the amplitude dispersion of the signal with respect to its average in a determinate time [Leon-Garcia-08], and it is given by:

$$VAR[X(t)] = \int_{-\infty}^{\infty} \left(x - m_x(t)\right)^2 f_{x(t)}(x)dx \tag{5-1}$$

where $m_x(t)$ is the mean function of the random process $X(t)$ and $f_{x(t)}(x)$ is the probability density function (PDF) of $X(t)$.

For the signal processing, a set $Y_1(n)$ consisting of a certain number of realizations, *WL*, is

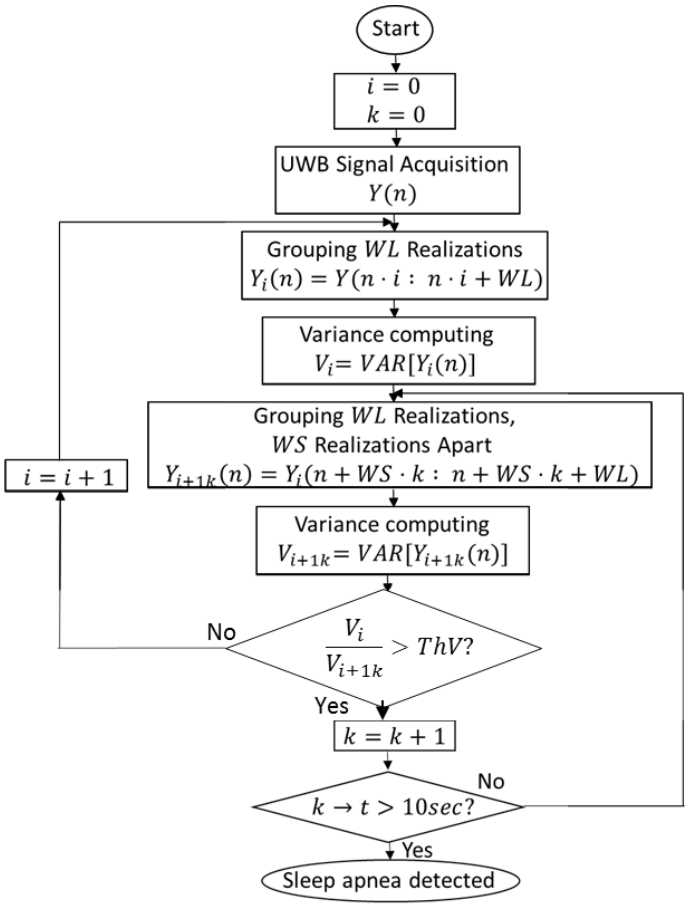

Fig. 5.1 Flowchart of the sleep apnea detection using the variance of realizations.

grouped into a "window" and its variance V_1 is calculated. A new window $Y_2(n)$ is analyzed by grouping other *WL* realizations located *WS* realizations apart from the start of the previous window: $Y_2(n) = Y_1(n + WS)$. Its variance is V_2. *WS* corresponds to the number of realizations or window step where the new window is defined. The construction of the grouping of realizations and window step is illustrated in Fig. 5.2.

This procedure, computing the variance of shifted windows, is executed continuously. The result is a signal containing the amplitude of variances, as it is shown in Fig. 5.3. In this figure, it is included a time interval when breathing ceased, and the amplitudes of the variances decreased abruptly. A comparison between consecutive variance amplitudes is also continuously computed, searching for this abrupt change by calculating:

$$r = \frac{V_1}{V_2} \tag{5-2}$$

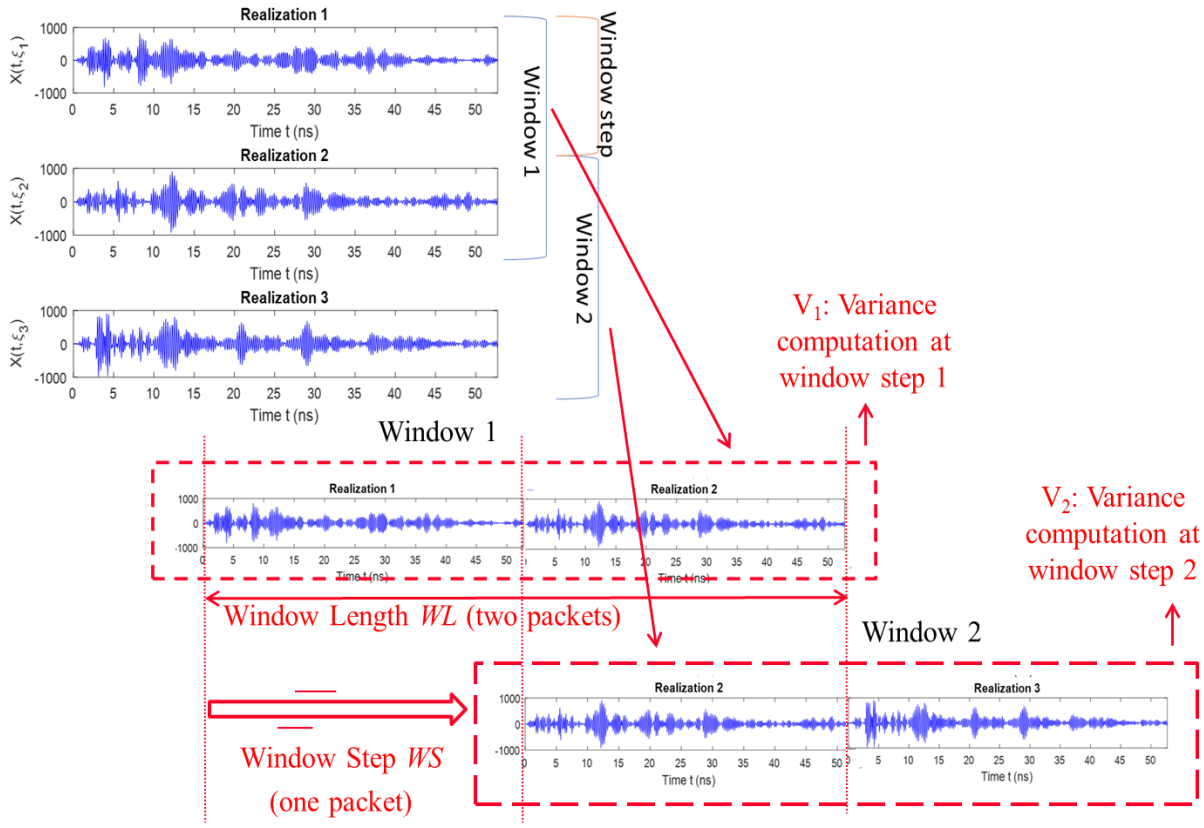

Fig. 5.2 Construction of realizations windows and definition of window step.

When the relation *r* between them is greater than a threshold value *ThV*, this point of time is considered as a potential start of apnea. Then, if the relation between subsequent variance amplitudes and the one at the start point is kept greater than the threshold value for more than 10 [Guyton-11], [Servin-Aguilar-18], apnea is declared. The computation of relation factor *r* for a signal lasting 60 seconds and an apnea at second 25 is shown in Fig. 5.4. Finally, when the relation *r* is lower than the threshold, then the patient is breathing again. This process is repeated until the complete signal is analyzed.

5.2. Results

In order to evaluate the performance of the algorithm, the same signals corresponding to

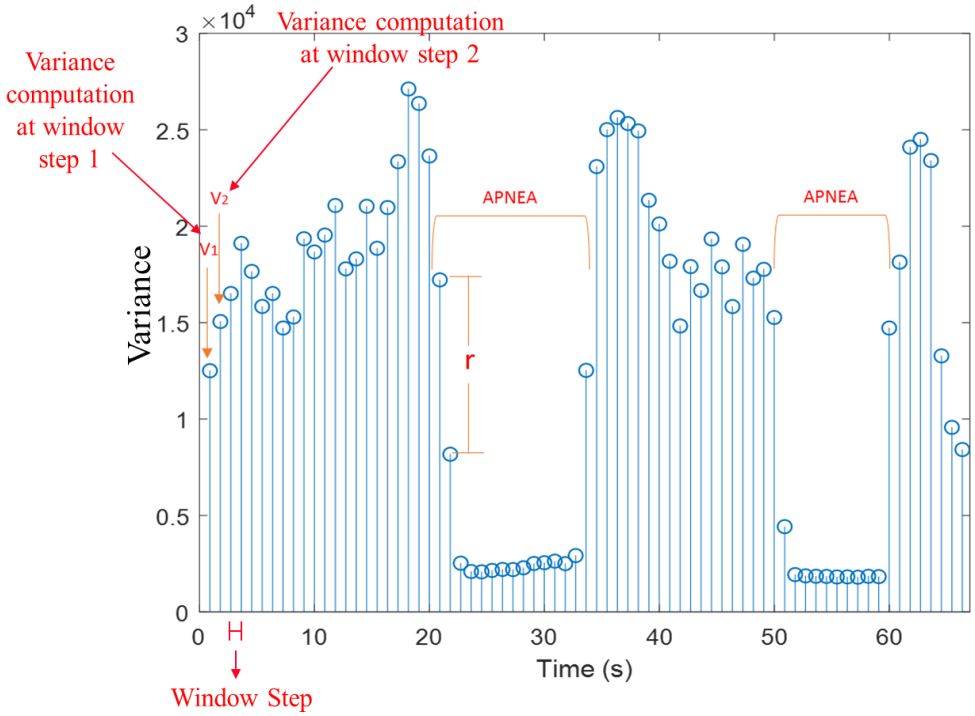

Fig. 5.3 Elements of variance computation by windows.

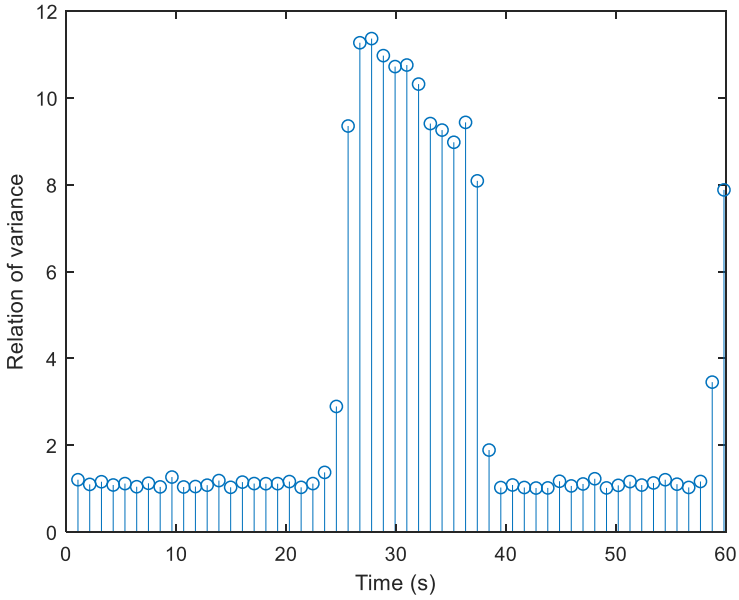

Fig. 5.4 Relation of variance amplitudes with a sleep apnea at second 25.

the experiments presented in the previous chapter are used. They were taken into two environments: a laboratory and a dormitory. In this part of the work, we use a UWB transceiver

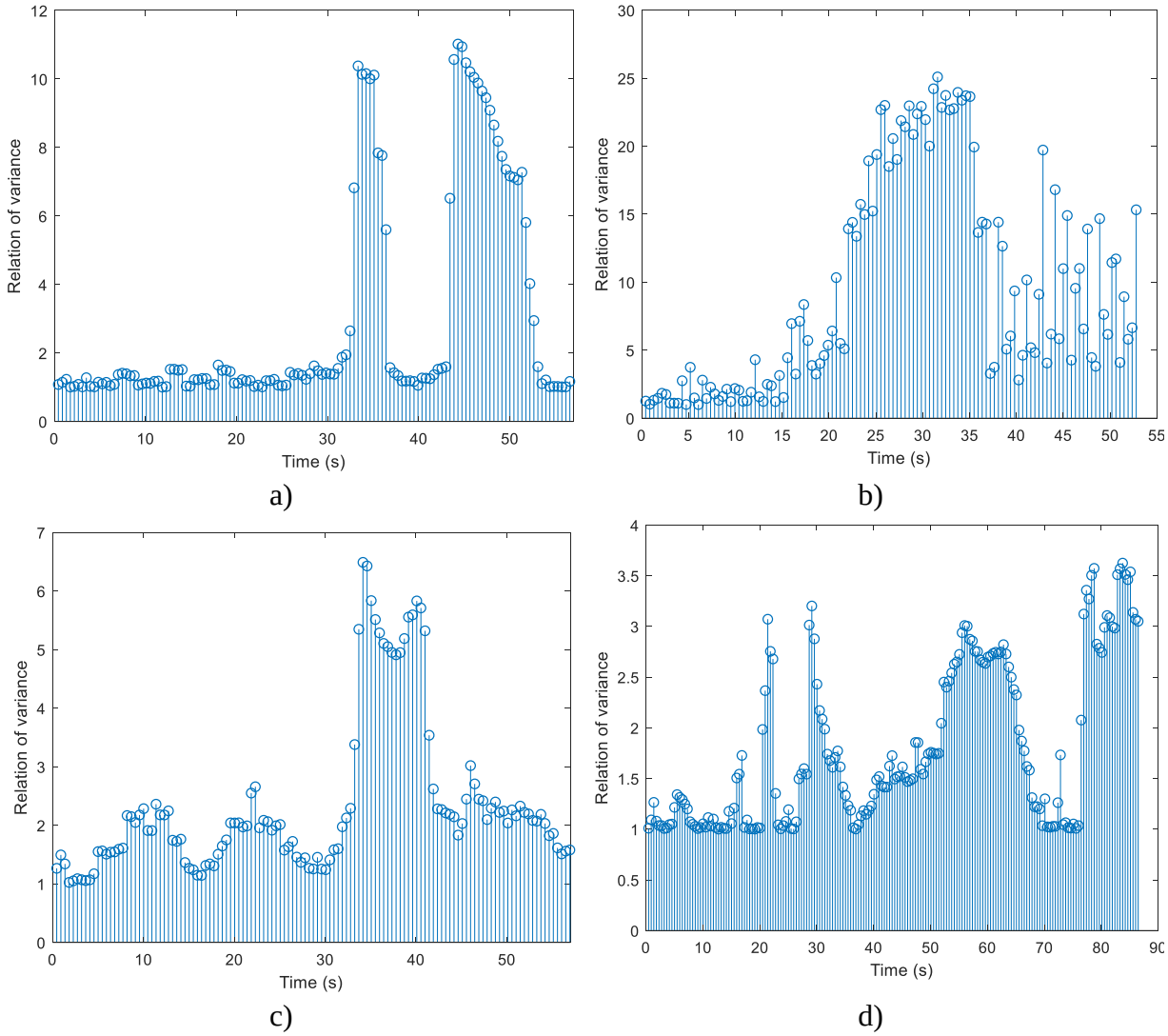

Fig. 5.5 Relation of variance amplitude for signals at different distances between the UWB device and the patient: a) 20 cm, b) 60 cm, c) 80 cm, and d) 100 cm.

acquiring signal realizations reflected from the human body at a frequency of 8 Hz.

In a first experiment, a signal acquired in a laboratory targeting directly to the chest of a patient is processed. The distance between the patient and the UWB transceiver is changed between 20 cm to 100 cm. Results are presented in Fig. 5.5 for values of comparison factor *r*.

In order to analyze the signal, a threshold ThV of 5 is chosen at four different distances and the sleep apnea is detected: 20 cm with an apnea at second 49 (Fig. 5.5a), 60 cm and an apnea at second 23 (Fig. 5.5b), 80 cm with an apnea at second 32 (Fig. 5.5c), and 100 cm with an apnea at second 50 (Fig. 5.5d). At distances greater than 100 cm, the signal is not suitable for processing.

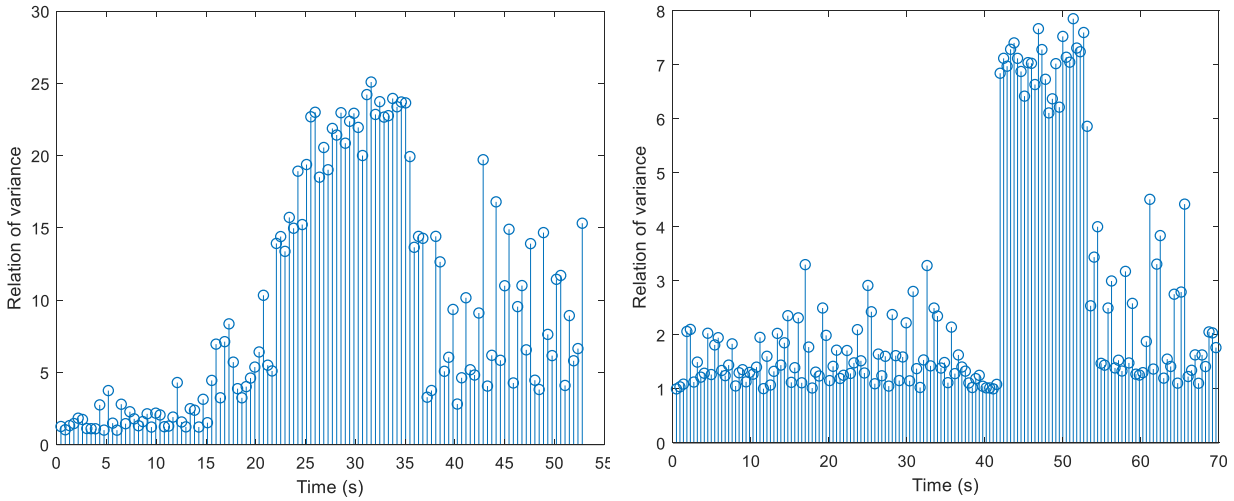

Fig. 5.6 Relation of variance amplitudes for signals in two scenarios: a) the patient is wearing a shirt, b) the patient is wearing a jacket.

When the threshold value ThV is changed to 2, then a sleep apnea is wrongly detected at second 50. If the distance between the UWB device and the patient is larger, then the threshold ThV must be lower to detect sleep apneas, because the amplitude of variances is smaller.

In a second experiment, the signal processed corresponds to a distance between the patient and the UWB transceiver of 60 cm and the patient wears two different clothes: a shirt and a jacket. The aim of this experiment is to evaluate the performance of the algorithm to detect sleep apneas when the patient is wearing different clothes. Results for the comparison factor *r* are shown in Fig. 5.6. When the patient wears a shirt, a sleep apnea occurring at second 23 is correctly detected using a ThV of 10, as shown in Fig. 5.6a. When the patient wears a jacket, a sleep apnea at second 42 is correctly detected with a threshold ThV of 3 (see Fig. 5.6b). It is seen that, while the clothes that the patient is wearing are irrelevant to detect the sleep apnea, the amplitude of the variance relation should be changed according to the patient clothes.

In a third experiment, the signal to process is acquired in a dormitory, where the patient is laying down on his side in a bed. The UWB device is addressed to the chest of the patient. Two scenarios are considered: the patient wearing a shirt and the patient covered with a thick blanket. Results of the comparison factor *r* are shown in Fig. 5.7. An apnea is present at second 45 for the patient wearing a shirt and the apnea is correctly detected (see Fig. 5.7a). When the patient is covered with a thick blanket (see Fig. 5.7b), a clear apnea is present at second 47 and is correctly

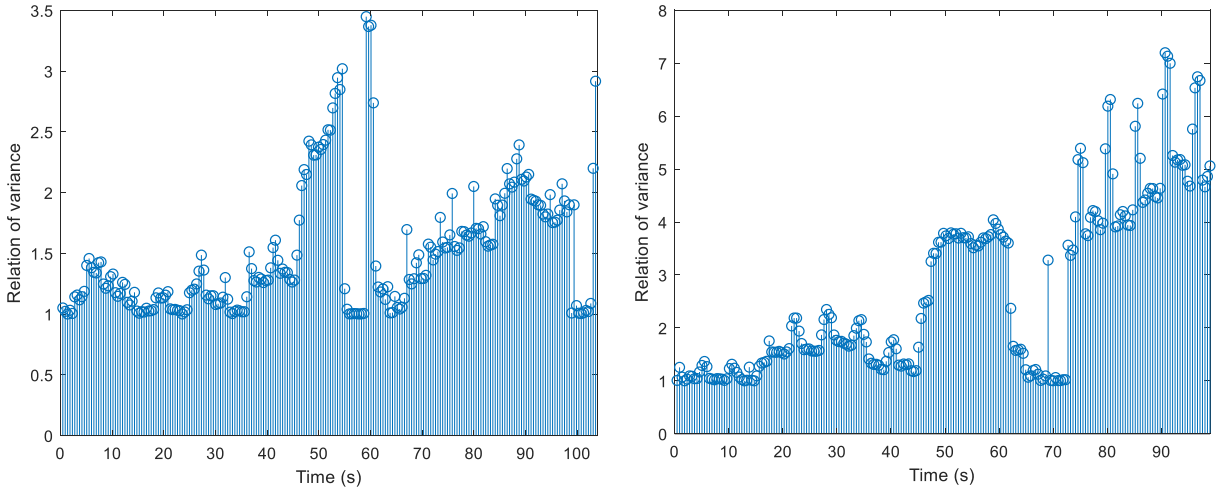

Fig. 5.7 Relation of variance amplitudes for signals in a dormitory: a) the patient is wearing a shirt, b) the patient is covered with a thick blanket.

detected, however, the results also indicate a second apnea at second 75, which does not exist. Then, it is important to improve and optimize the parameters that the algorithm uses to detect the sleep apnea more accurately.

5.3. Optimization Methodology

In order to find the conditions with the best performance of the proposed apnea detection method, the main parameters involved in the computation are changed in a series of executions of the algorithm. The targeted parameters are the window length, *WL*, the shift or step between consecutive windows, *WS*, and the threshold value, *ThV*.

The experiments, carried out over a UWB signal corresponding to the chest movement of the patient, have two main objectives. First, to evaluate the parameters that produce the best accuracy of the apnea detection method. Second, to identify the parameters with shortest processing time.

The proposed optimization methodology essentially consists of a parametric multidimensional search based on actual physical measurements. Each execution of the searching process begins with the values of two parameters fixed, *WL* and *WS*, being the threshold value varied. Once the whole process of detection over the signal is carried out, a new execution is run

TABLE 5.1. NUMBER OF COMBINATIONS OF PARAMETERS THAT PRODUCED CORRECT DETECTIONS

Signal Characteristics		Number of Correct Detections
Number of Apneas	Distance between the UWB Transceiver and the Patient (cm)	
0	60	17,731
1	20	1,291
1	30	2,383
2	30	1,564
1	80	866

by fixing *WL* and *WS* to new values and then varying *ThV*. The executions are repeated by modifying the parameters until their ranges of variation are covered. For each execution, the values of the parameters, the number of detected apneas, and the processing time are saved.

5.4. Optimization Results

The set of experiments are performed over five signals presenting different characteristics. Each signal corresponds to a series of around 750 realizations, lasting 94 seconds in total. As a reference for the experiments, the average breathing frequency of a patient is considered to be 0.2 Hz or 5 seconds. The parameter ranges considered are: for the window length *WL*, from 4 realizations, which represents 0.5 seconds, to 128 realizations, corresponding to 16 seconds; for the window step *WS*, from 1 realization to the maximum length of the window; and for the threshold value *ThV*, from 1 to 10. This makes a total of 18,544 combinations of parameters tested for each signal.

The difference between the signals used in the experiments are the number of apneas and the distance between the UWB transceiver and the patient. Table 5.1 shows the characteristics of the signals and the number of combinations of parameters that presented a correct detection out of the 18,544 possible combinations. Table 5.2 - Table 5.6 show, for each signal, a subset of the values of the parameters with correct detections. They are a subset of combinations chosen in a way that allows to identify the ranges of common values between the 5 signals.

The first signal used has a length of 85.63 seconds with zero apneas and a distance between

TABLE 5.2. DETECTION RESULTS FOR SEVERAL PARAMETERS USING A SIGNAL WITHOUT APNEAS, ACQUISITION DISTANCE = 60 CM, LENGTH = 85.63 SECONDS

PARAMETERS		
WL	*WS*	*ThV* Range
16	10	2.5 – 10
16	11	2.5 – 10
16	12	2.5 – 10
16	13	2.5 – 10
16	14	2.5 – 10
24	12	2 – 10
24	13	2 – 10
24	14	2 – 10
24	15	2 – 10
24	16	2 – 10
32	14	1.5 – 10
32	16	1.5 – 10
32	18	2 – 10
32	25	2 – 10
32	27	1.5 – 10
40	12	1.5 – 10
40	13	1.5 – 10
40	14	1.5 – 10
40	15	1.5 – 10
40	16	1.5 – 10

the UWB device and the patient of 60 cm. A total of 17,731 combinations correctly detected the absence of apneas (see Table 5.1). The detection results for this first signal are in Table 5.2, showing a subset of these combinations, where *WL* has a range from 16 to 40 realizations, *WS* varies from 10 to 27, and *ThV* presents a maximum range from 1.5 to 10.

The second signal used has a length of 81.3 seconds with one apnea and a distance of 20 cm. The number of combinations that detected correctly the apnea is 1,291 (see Table 5.1). From the subset shown in Table 5.3, it is seen that the range for the *WL* parameter is from 8 to 40 realizations, the *WS* range is from 8 to 19, and the value of *ThV* varies from 1 to 10.

TABLE 5.3. DETECTION RESULTS FOR SEVERAL PARAMETERS USING A SIGNAL WITH ONE APNEA, ACQUISITION DISTANCE = 20 CM, LENGTH = 81.3 SECONDS

PARAMETERS		
WL	*WS*	*ThV* Range
8	8	2.5 – 10
16	8	6 – 10
16	9	3.5 – 4.5
16	10	1 – 9
16	11	1 – 4.5
24	12	1 – 4.5
24	13	1 – 6.5
24	14	1 – 6
24	15	1 – 5
24	16	1 – 5.5
32	13	1 – 5
32	14	1 – 5
32	15	1 – 4.5
32	16	1 – 4.5
32	17	1 – 2.5
40	15	1 – 4.5
40	16	1 – 4
40	17	1 – 3.5
40	18	1 – 4.5
40	19	1 – 4

The third signal has a length of 113.4 seconds. It has one sleep apnea and an acquisition distance of 30 cm. The number of correct detections is 2,383 combinations (see Table 5.1). It is shown in Table 5.4 that *WL* has a range from 16 to 40, the *WS* range is from 11 to 15, and the *ThV* maximum range is from 1 to 10.

The fourth analyzed signal has a length of 89.5 seconds, with two apneas, and an acquisition distance of 30 cm. The total number of combinations producing correct detections is 1,564 (see Table 5.1). In this experiment, the subset of combinations of parameters shown in Table 5.5 corresponds to *WL* with a range from 16 to 40 realizations, *WS* from 9 to 17, and *ThV* with a

TABLE 5.4. DETECTION RESULTS FOR SEVERAL PARAMETERS USING A SIGNAL WITH ONE APNEA, ACQUISITION DISTANCE = 30 CM, LENGTH = 113.4 SECONDS

PARAMETERS		
WL	*WS*	*ThV* Range
16	11	1 – 10
16	12	1 – 7.5
16	13	2 – 10
16	14	2 – 7
16	19	1 – 10
24	11	2 – 9.5
24	12	2 – 7
24	13	2 – 9
24	14	2 – 7
24	15	2 – 9.5
32	11	2 – 8
32	12	2 – 6.5
32	13	2 – 8
32	14	2 – 6.5
32	15	2 – 7.5
40	11	2 – 7
40	12	2 – 5.5
40	13	1 – 7
40	14	2 – 5.5
40	15	1 – 7

variation from 1.5 to 8.

Finally, the fifth experiment has a length of 118.3 seconds, with one apnea, and an acquisition distance of 80 cm. In this experiment, the total number of correct detections is obtained from 866 combinations (see Table 5.1). The range of *WL* is from 48 to 72 realizations, *WS* varies from 8 to 40 realizations, and *ThV* range is from 1.5 to 6, as seen in Table 5.6. In this case, it is found that the ranges of parameters values stepped away from the group of values obtained in the previous results.

The few coincident results of the fifth signal, in comparison with the first four signals, show

TABLE 5.5. DETECTION RESULTS FOR SEVERAL PARAMETERS USING A SIGNAL WITH TWO APNEAS, ACQUISITION DISTANCE = 30 CM, LENGTH = 89.5 SECONDS

PARAMETERS		
WL	*WS*	*ThV* Range
16	9	2.5 – 4
16	10	1.5 – 3
16	11	1.5 – 3
16	12	1.5 – 8
16	13	1.5 – 4.5
24	12	1.5 – 7
24	13	1.5 – 5
24	14	1.5 – 8
24	15	1.5 – 7
24	16	1.5 – 5.5
32	12	1.5 – 6
32	13	1.5 – 5
32	14	1.5 – 6.5
32	15	1.5 – 6.5
32	16	1.5 – 6.5
40	13	1.5 – 4.5
40	14	1.5 – 5.5
40	15	1.5 – 5.5
40	16	1.5 – 5.5
40	17	1.5 – 5

that the distance has an important effect in the detection algorithm. In addition, it is also observed that the number of correct detections decreased by half. In this case, we cannot define a range of parameters values good enough for all tested signals. We conclude that the signal tested at a distance of 80 cm is not suitable for the proposed algorithm, since it makes the algorithm unreliable.

Taking into account the results obtained for the first four signals, we can determine an appropriate set of reliable values, valid for all four signals. This set comprises a *WL* equal to 24, a *WS* ranging from 12 to 15 realizations and a *ThV* range from 2 to 4.5. This means that these selected

TABLE 5.6. DETECTION RESULTS FOR SEVERAL PARAMETERS USING A SIGNAL WITH ONE APNEA, ACQUISITION DISTANCE = 80 CM, LENGTH = 118.3 SECONDS

PARAMETERS		
WL	*WS*	*ThV* Range
16	9	2.5 – 4
16	10	1.5 – 3
16	11	1.5 – 3
16	12	1.5 – 8
16	13	1.5 – 4.5
24	12	1.5 – 7
24	13	1.5 – 5
24	14	1.5 – 8
24	15	1.5 – 7
24	16	1.5 – 5.5
32	12	1.5 – 6
32	13	1.5 – 5
32	14	1.5 – 6.5
32	15	1.5 – 6.5
32	16	1.5 – 6.5
40	13	1.5 – 4.5
40	14	1.5 – 5.5
40	15	1.5 – 5.5
40	16	1.5 – 5.5
40	17	1.5 – 5

values can be used for the detection of apneas within the first four signals. On the other hand, it can easily be found that, for a fixed value of parameter *WL*, the minimum number of operations to be computed is obtained when the value of *WS* is the largest. We can then define that the *WS* value to be used for all tested signals is 15. In summary, we conclude that a set of values that allows the detection algorithm to have a good performance with the least number of calculations, is a *WL* of 24, a *WS* of 15 and a range *ThV* from 2 to 4.5.

5.5. Conclusions

An algorithm to detect sleep apnea using the relation of the variance of signals obtained from a UWB transceiver was presented in this chapter. It was demonstrated that the algorithm detects the sleep apnea with a maximum distance of 100 cm between the UWB device and the patient. The experiments also showed that the algorithm is able to detect sleep apnea considering different scenarios, with some limitations. Since the performance of the algorithm depends on some parameters, additional studies are necessary to find their optimal values for a more effective performance.

An optimization methodology to improve a sleep apnea detection system that computes the variance of the signal reflected from the patient's chest was also presented in this chapter. The experimental evaluation allowed to identify the combinations of parameters that produce the best results and the smallest number of operations. The parametric optimization of the algorithm showed that the best detection results were achieved by using a *WL* of 24 realizations, *WS* of 15 realizations, and a *ThV* between 2 and 4.5. It was also found that the detector was not accurate at a distance of 80 cm between the UWB device and the patient.

General Conclusions

This doctoral dissertation has shown how the processing of vital signs can help detecting diseases, in the context of remote monitoring of patients. This means that the processing must consider few resources at the remote site: low power consumption and low computing power.

In Chapter 1, an overview of different biomedical signals, such as ECG or EEG signals, was presented. In addition, different techniques to reduce the energy consumption in devices that work in WSN and/or WBAN for healthcare applications were studied. We identified the opportunity to contribute studying the processing of vital signals with an energy efficiency point of view.

In Chapter 2, the compression technique was considered as a method to reduce the energy consumption when a signal is transmitted. The selected method to test was the wavelet transform, which divides the signal in different band frequencies isolating the desired frequency. In this chapter, the EEG signal was compressed using different wavelet families. Here, the performance of every selected family was compared using two different criteria (NMSE and PRD). The Coiflets family presented the best compression ratio (88% of the original signal) for the case $j = 4$, while the Haar family presented an adequate performance related to the NMSE and PRD criteria. The literature reported that the Coiflets family could be used to detect features of an EEG signal. However, the results presented in this chapter showed that the Haar family had a better performance than the Coiflets family.

In Chapter 3, an accurate epileptic seizure detector using the EEG signal was presented, characterizing the EEG signal as a heavy-tail distribution. The EEG tail tends to decay similarly to a Pareto distribution, so a detector that uses alpha-stable parameters was designed. It is shown that when an epileptic seizure occurs, the gamma parameter presents significant changes that can help to detect the disorder. In addition, three estimators to calculate the gamma parameter are evaluated (McCulloch, Stablekull, and Nolan estimators), resulting that Nolan was the one with the best performance. It can be shown that the proposed algorithm is more sensitive than others reported in the literature and the processing time of the algorithm is shorter. Results show that the best performance is obtained with a window-length of 1.95 seconds. Regarding the window-length in the smoother block, the best performance is obtained when the length is 0.03 seconds. Finally,

the overall processing time required to analyze the complete EEG signal is 0.1725 seconds for a 30 minutes long EEG signal.

In Chapter 4, an automatic technique to detect the breathing signal based on the variance of a UWB signal reflecting on a person was presented. This let to define a sleep apnea detector that was tested in different patients and environments effectively. Two methods were considered to analyze the signal and detect the sleep apnea: the correlation and the derivative of the signal. The proposed algorithm showed a good performance in general; within a 100-cm range, both the sleep apnea and the breathing frequency were detected efficiently.

Finally, in Chapter 5, a method to detect sleep apnea using the relation of the variance of signals with an UWB transceiver is presented. This method does not require the previous calculation of the breathing signal. Results showed that the algorithm is able to detect sleep apnea considering different scenarios, with some limitations. After testing the algorithm, an optimization is performed in order to reduce the number of calculations. The optimization results allowed to identify the combination of parameters that produce the best results and the smaller number of operations. We detected that the best detection was obtained when we used a *WL* of 24 realizations, *WS* of 15 realizations and *ThV* between 2 and 4.5. It was also found that the detector was not accurate at a distance of 80 cm or more between the UWB device and the patient, making the proposed unreliable under those circumstances.

For future work regarding epilepsy detection, more experiments with different noise distribution will be considered in order to detect the epileptic seizures trying to simulate a more realistic noise behavior. A new non-invasive method to detect the EEG signal of a patient without placing electrodes in his scalp face will be considered.

Concerning the sleep apnea section, new experiments considering two UWB devices will be performed. They will be located in different points of the room in order to guarantee the accuracy of the sleep apnea detection in a patient when he is asleep. A filter structure to characterize the signal spectrum and every parameter associated to the physical signal will be designed.

More tests will be performed considering more patients in a real environment.

Conclusiones Generales

Esta tesis presenta cómo el procesamiento de los signos vitales de un paciente puede ayudar a detectar enfermedades, en el contexto del monitoreo remoto de sus condiciones de salud. Esto implica que el procesamiento debe tomar en cuenta características como un bajo consumo de energía y un poder de cómputo disminuido.

En el Capítulo 1, se realizó un estudio general de diferentes señales biomédicas, como las señales de ECG y EEG. Adicionalmente, se estudiaron diferentes técnicas para reducir el consumo de energía en dispositivos que trabajan en redes WSN y WBAN para aplicaciones de la salud. Se identificó como una oportunidad de contribución el análisis de las señales vitales de un paciente desde un punto de vista de reducir el consumo energético.

En el Capítulo 2, se consideró la compresión de señal como un método para reducir el consumo de energía cuando se transmite una señal. En este trabajo, se usó la transformada wavelet, que divide la señal en sus diferentes bandas de frecuencia y aísla la frecuencia deseada para ser transmitida. En este capítulo, una señal de EEG fue comprimida usando diferentes familias wavelet, comparándolas bajo dos diferentes criterios (NMSE y PRD). Los resultados mostraron que la familia Coiflets mostró la mejor taza de compresión (88% de la señal original) cuando se tiene una $j = 4$, mientras que la familia Haar presentó un desempeño adecuado en relación a los criterios NMSE y PRD. En la literatura se reporta que la familia Coiflets es usada para caracterizar una señal de EEG. Sin embargo, los resultados presentados en este capítulo muestran que la familia Haar tiene mejor desempeño que la familia Coiflets.

En el Capítulo 3, se muestra el desarrollo de un detector de ataques epilépticos usando señales de EEG, basándose en la caracterización de la señal EEG como una señal con distribución de cola pesada. Ésta tiende a decaer de forma similar a la distribución de Pareto, por lo que se diseñó un detector usando parámetros alfa-estables. Se muestra que cuando ocurre un ataque epiléptico, el parámetro gama muestra un cambio significativo que ayuda a detectar la enfermedad. Adicionalmente, tres estimadores son evaluados (los estimadores de McCulloch, Stablekull y Nolan), resultando que el estimador de Nolan tuvo el mejor desempeño, mostrando que el algoritmo propuesto tiene una mejor sensibilidad que otros reportados en la literatura y el tiempo de procesamiento del algoritmo es más corto. Los resultados muestran que el mejor desempeño se

obtuvo cuando la ventana de análisis de la señal de EEG tiene una longitud de 1.95 segundos. Ahora, el mejor desempeño en el bloque suavizador se obtuvo cuando la longitud del deslizamiento de la ventana es de 0.03 segundos. Finalmente, el tiempo total de procesamiento que requiere el algoritmo para analizar una señal de EEG de 30 minutos es de 0.1725 segundos.

En el Capítulo 4 se presenta una técnica automática para detectar la señal de la respiración de un paciente a través de la varianza y la detección de la apnea del sueño. El algoritmo fue probado en diferentes pacientes y ambientes de forma efectiva. El algoritmo propuesto muestra un buen desempeño en términos de distancia y tiempo de procesamiento, dentro de un rango de 100 metros, la apnea del sueño y la frecuencia de respiración fueron detectadas correctamente. Aquí, dos métodos fueron considerados para detectar la apnea del sueño (la correlación y la derivada de la señal). En ambos casos la apnea del sueño fue detectada correctamente.

Finalmente, en el Capítulo 5, se muestra un método para detectar la apnea del sueño usando la relación de la varianza de la señal con un transductor UWB. Los resultados mostraron que el algoritmo detectó la apnea del sueño en diferentes escenarios, con algunas limitaciones. Después de probar el algoritmo, se optimizó con el objetivo de reducir el número de operaciones requeridas. La optimización permitió encontrar los mejores valores de los parámetros del algoritmo que produjeran la menor cantidad de operaciones posible. Se detectó que el mejor rendimiento fue obtenido cuando WL es de 24 realizaciones, WS de 15 realizaciones y el umbral ThV está entre 2 y 4.5.

El trabajo a futuro considera, en relación a la detección de epilepsia, la realización de más experimentos, tomando en cuenta diferentes tipos de ruidos, de manera tal que se puedan detectar ataques epilépticos simulando un comportamiento del ruido más similar al real. Por otra parte, se considerará el estudio de un nuevo método no invasivo para detectar señales de EEG en el paciente, sin poner electrodos en el cuero cabelludo.

En lo que se refiere a la apnea del sueño, se realizarán experimentos empleando dos dispositivos UWB. Estos serán colocados en diferentes puntos de un cuarto, con el fin de garantizar una detección más precisa de la apnea del sueño cuando el paciente está dormido. El diseño de un filtrado estructurado para caracterizar el espectro de cada uno de los parámetros asociados a las señales físicas será considerado.

Más pruebas se realizarán considerando pacientes en entornos reales.

Appendix

A. LIST OF INTERNAL RESEARCH REPORTS

1) J. G. Servin-Aguilar, L. Rizo-Dominguez, and J. A. Pardiñas-Mir, "An overview of energy efficiency in wireless sensor area networks for health care applications," Internal Report *PhDEngScITESO-14-11-R*, Tlaquepaque, Mexico, Dec. 2014.

2) J. G. Servin-Aguilar, L. Rizo-Dominguez, and J. A. Pardiñas-Mir, "Signal analysis using wavelet transform," Internal Report *PhDEngScITESO-15-23-R*, Tlaquepaque, Mexico, Dec. 2015.

3) J. G. Servin-Aguilar, L. Rizo-Dominguez, and J. A. Pardiñas-Mir, "A comparison between wavelet families to compress an EEG signal," Internal Report *PhDEngScITESO-16-32-R*, Tlaquepaque, Mexico, Dec. 2016.

4) J. G. Servin-Aguilar, J. A. Pardiñas-Mir, and L. Rizo-Dominguez, "Breathing signal and sleep apnea detection using UWB technology," Internal Report *PhDEngScITESO-17-40-R*, Tlaquepaque, Mexico, Nov. 2017.

5) J. G. Servin-Aguilar, J. A. Pardiñas-Mir, and L. Rizo-Dominguez, "Obtaining the breathing signal from UWB signals," Internal Report *PhDEngScITESO-17-45-R*, Tlaquepaque, Mexico, Dec. 2017.

6) J. G. Servin-Aguilar, J. A. Pardiñas-Mir, and L. Rizo-Dominguez, "Alpha-stable parameters to describe a heavy tail distribution," Internal Report *PhDEngScITESO-18-06-R*, Tlaquepaque, Mexico, Apr. 2018.

7) J. G. Servin-Aguilar, J. A. Pardiñas-Mir, and L. Rizo-Dominguez, "Epilpetic seizure detector using the gamma parameter of an alpha-stable estimator," Internal Report *PhDEngScITESO-18-18-R*, Tlaquepaque, Mexico, May 2018.

8) J. G. Servin-Aguilar, J. A. Pardiñas-Mir, and L. Rizo-Dominguez, "Sleep Apnea detector through the variance for UWB signals reflecting on a human body," Internal Report *PhDEngScITESO-18-26-R*, Tlaquepaque, Mexico, Sep. 2018.

9) J. G. Servin-Aguilar, J. A. Pardiñas-Mir, and L. Rizo-Dominguez, "Optimization of the sleep apnea detection using UWB signals variance," Internal Report *PhDEngScITESO-18-30-R*, Tlaquepaque, Mexico, Nov. 2018.

B. LIST OF PUBLICATIONS AND INTELECTUAL PROPERTY

B.1. CONFERENCE PAPERS

1) J. G. Servín-Aguilar, L. Rizo-Dominguez, and J. A. Pardiñas-Mir, "A comparison between wavelet families to compress an EEG signal," in *IEEE ANDESCON Proc.*, Arequipa, Peru, Oct. 2016, pp. 1-4. (ISBN: 978-1-5090-2532-9; e-ISBN: 978-1-5090-2533-6; INSPEC: 16650402; DOI: 10.1109/ANDESCON.2016.7836192).

2) J. G. Servín-Aguilar, M. Muller, G. Abib, J. A. Pardiñas-Mir, and L. Rizo-Dominguez, "System to detect sleep apnea syndrome using the signal similarity," in *Int. Conf. Electrical, Electronics, Computers, Communication, Mechanical, and Computing (EECCMC)*, Tamil Nadu, India, Jan. 2018, pp. 1-6.

B.2. PATENTS

1) J. G. Servín-Aguilar, L. Rizo-Domínguez, and J. A. Pardiñas-Mir (ITESO), "Sistema de alertas para el aviso de epilepsia," Mexican Patent Application MX/A/2018/003153 (IMPI), March 14, 2018.

Bibliography

[AASM-17] American Academy of Sleep Medicine. (2017). *New Guideline for Diagnostic Testing for Adult Sleep Apnea (rev. Mar. 10)* [Online]. Available: http://www.aasmnet.org/articles.aspx?id=6792.

[Abib-14] G. I. Abib, M. Muller, C. Seoane-Gomez, and P. Fernandez-Sepulveda, "Ultra-wideband RADAR system for range measurement," *in IEEE International Conference on Ultra-WideBand (ICUWB)*, Paris, France, Nov. 2014, pp. 197-201.

[Abualsaud-13] K. Abualsaud, M. Mahmuddin, R. Hussein, and A. Mohamed, "Performance evaluation for compression-accuracy trade-off using compressive sensing for EEG-based epileptic seizure detection in wireless tele-monitoring", *IWCMC Conf.*, Sardinia, Italy, July 2013, pp 231-236.

[Adler-98] R. J. Adler, R. E. Feldman, and M. S. Taqqu, *A Practical Guide to Heavy Tails: Statistical Techniques and Applications*. Berlin, Germany: Birkhauser Editions, 1998.

[Anderson-98] P. L. Anderson and M. M. Meerschaert, "Modeling river flows with heavy tails," *Water Resources Research Journal*, vol. 34, no. 9, pp. 2271-2280, Sep. 1998.

[Awad-13] A. Awad, R. Hussein, A. Mohamed, and A.A. El-Sherif, "Energy-aware cross-layer optimization for EEG-based wireless monitoring applications", *LCN Conf.*, Sydney, Australia, Oct. 2013, pp. 356-363.

[Bates-97] S. Bates and S. McLaughlin, "The estimation of stable distribution parameters," in *HOST Conf.*, Banf, Canada, Jul. 1997, pp. 390 – 394.

[CDC-17] Centers for Disease, Control, and Prevention. (2018). *Health and Economic Costs of Chronic Disease (rev. Mar. 18)* [Online]. Available: https://www.cdc.gov/chronicdisease/about/costs/index.htm.

[CODES-16] Experiment codes (2016, January 25), *Citation* [Online]. Available: https://sites.google.com/sites/researchbyzhang/bsbl.

[Fedele-15] G. Fedele, E. Pittella, S. Pisa, M. Cavagnaro, R. Canali, and M. Biagi, "Sleep-apnea detection with UWB active sensors," *in IEEE International Conference on Ubiquitous Wireless Broadband (ICUWB)*, Montreal, Canada, Oct. 2015, pp. 1-5.

[Gandhi-11] T. Gandhi, B. K. Panigrahi, and S. Anand, "A comparative study of wavelet families for EEG signal classification", *Neurocomputing Journal*, vol. 74, no. 17, pp. 3051-3057, Oct. 2011.

[Guyton-11] A. C. Guyton and J. E. Hall, *Tratado de Fisiología Médica*, Mexico: Elsevier Saunders, 2011.

[Hossain-12] M.A. Hossain and D.T. Ahmed, "Virtual caregiver: an ambient-aware elderly monitoring system*", IEEE Transactions on Information Technology in Biomedicine*, vol. 16, pp. 1024-1031, Nov. 2012.

[Huo-09] H. Huo, Y. Xu, H. Yan, S. Mubben, and H. Zhang, "An elderly health care system using wireless sensor networks at home", *SENSORCOMM Conf.* Glyfana, Athens, Jun. 2009, pp. 158-163.

BIBLIOGRAPHY

[Hussein-13] R. Hussein, A. Awad, A.A. El-Sherif, A. Mohamed, and M. Alghoniemy, "Adaptive energy-aware encoding for DWT-based wireless EEG tele-monitoring system", *DSP/SPE Meeting*, Napa, CA, Aug. 2013, pp. 245-250.

[IMSS-15] IMSS (2015, Jan. 29) *Informe al ejecutivo federal y al H. congreso de la unión 2012-2013* [Online] Available: http://www.imss.gob.mx/sites/all/statics/pdf/informes/20122013/Introduccion.pdf.

[Jian-05] Z. Jian, Y. Ning, B. An, A. Li, and H. Feng, "Detecting mental EEG properties using detrended fluctuation analysis," in *IEMBS Conf.*, Shangai, China, Jan. 2005, pp. 2017-2020.

[Kannan-13] S.S. Kannan and N.S. Varsha, " Wireless telemonitoring of wearable device for recording biopotentials using embedded terminal platform", *ICCSP Conf.*, Melmaruvathur, India, April 2013, pp. 918-921.

[Karli-16] R. Karli, H. Ammor, R. M. Shubair, M. I. AlHajri, R. Alkurd, and A. Hakam, "Miniature planar ultra-wide-band microstrip antenna for breast cancer detection," *in Mediterranean Microwave Symposium (MMS)*, Abu Dhabi, United Arab Emirates, Nov. 2016, pp. 1-4.

[Leon-Garcia-08] A. Leon-Garcia, *Probability, Statistics, and Random Process for Electrical Engineering*, Third Edition, Upper Sandler River, NJ: Pearson Prentice-Hall, 2008.

[Liu-13] B. Liu, Z. Zhang, H. Fan, and Q. Fu, "Compression via compressive sensing: a low-power framework for the telemonitoring of multi-channel physiological signals", *BIBM Conf.*, Shanghai, China, Dec. 2013, pp. 9-12.

[Mallat-99] S. Mallat, *A Wavelet Tour of Signal Processing*, San Diego, CA: Academic Press, 1999.

[Mamaghanin-11] H. Mamaghanian, N. Khaled, D. Atienza, and P. Vandergheysnt, "Compressed sensing for real-time energy-efficient ECG compression on wireless body sensor nodes", *IEEE Transactions on Biomedical Engineering*, vol. 58, no. 9, pp. 2456-2466, Sep. 2011.

[Manolakis-05] D. G. Manolakis, V. K. Ingle, and S. M. Kogon, *Statistical and Adaptive Signal Processing, Spectral Estimation, Signal Modeling, Adaptive Filtering, and Array Processing*. Norwood, MA: Artech House, 2005.

[Marzbani-16] H. Marzbani, H. R. Marateb, and M. Mansourian, "Neurofeedback: a comprehensive review on system design, methodology, and clinical applications," *Basic and Clinical Neuroscience Journal*, vol. 7, no. 2, Apr. 16, pp. 143-158.

[MATLAB-16a] MatLab function. (2016). *Estimation of Alpha-Stable Distribution Parameters Using a Quantile Method* (rev. Jan. 10) [Online]. Available: https://www.mathworks.com/matlabcentral/fileexchange/34783-estimation-of-alpha-stable-distribution-parameters-using-a-quantile-method.

[MATLAB-16b] MatLab function. (2016). *Stablecull: MATLAB Function to Estimate Stable Distribution Parameters Using the quantile Method of McCulloch* (rev. Jan. 10) [Online]. Available: https://ideas.repec.org/c/boc/bocode/m429006.html.

[McCulloch-86] J. H. McCulloch, "Simple consistent estimators of stable distribution parameters," *Communications on Statistics – Simulation and Computational*, vol. 15, no. 4, pp. 1109-1136, Jan. 1986.

[MEDLINE-17] MedlinePlus. (2017). *Sleep Apnea (rev. Mar. 10)* [Online]. Available: https://medlineplus.gov/sleepapnea.html.

[MIT-14] MIT database. (2014). *Scalp EEG Database* (rev. Nov. 03) [Online]. Available: https://www.physionet.org/pn6/chbmit/.

[Muller-15] M. Muller and G. I. Abib, "Ultra WideBand RADAR system for human chest displacement," in *IEEE 13th International New Circuits and Systems Conference (NEWCAS)*, Grenoble, France, Aug. 2015, pp. 1-4.

[Nefti-10] S. Nefti, U. Manzoor, and S. Manzoor, "Cognitive agent based intelligent warning system to monitor patients suffering from dementia using ambient assisted living", *i-Society Conf.*, London, England, Jun. 2010, pp. 92-97.

[NHLBI-17] National Heart, Lung, and Blood Institute. (2017). *Sleep apnea* (*rev. Mar. 17*) [Online]. Available: https://www.nhlbi.nih.gov/health/health-topics/topics/sleepapnea/.

[Pardiñas-Mir-09] J. A. Pardiñas-Mir, "Ultra-wideband communications and the TDSC detection method," Technical Report *Department of Electronics, Systems and Informatics, ITESO University*, Tlaquepaque, Mexico, Mar. 2009.

[Pardiñas-Mir-12] J. A. Pardiñas-Mir, *Contribution à l'etude de la detection des signaux UWB. Etude et implementation d'un récepteur ad hoc multicapteurs. Applications indoor de localisation*, These de Doctorat, EDITE de Paris, Paris, France, 2012.

[Perez-Sevilla-97] J. J. Perez-Sevilla, *Compresión de la Señal de Electrocardigrafía basada en el Análisis de Ondeleta e Implementación en un Procesador de Señales*, Master Thesis, Laboratory of Electrical Engineering and Computational Science, CINVESTAV, Guadalajara, Mexico, 1997.

[Ramgopal-14] S. Ramgopal, S. Thome-Souza, M. Jackson, N. E. Kadish, I. S. Fernandez, J. Klehm, W. Bosl, C. Reinsberger, S. Schachter, and T. Loddenkemper, "Seizure detection, seizure prediction, and close-loop warning systems in epilepsy", *Epilepsy & Behavior Journal*, vol. 37, pp. 291-307, Jun. 2014.

[Sahambi-97] J. S. Sahambi, S.N. Tandon, and R.K.P. Bhatt, "Using wavelet transform for ECG characterization. An on-line digital signal processing system," *IEEE Engineering in Medicine and Biology Magazine*, vol. 16, pp. 77-83, Jan. 1997.

[Sayood-00] K. Sayood, *Introduction to Data Compression*, second edition, San Francisco, Ca: Morgan Kaufmann Publishers, 2000.

[Salas-Gonzalez-14] D. Salas-Gonzalez, J. M Gorriz, J. Ramirez, and E. W. Lang, "Why using the alpha-stable distribution in neuroimage?," in *SIGMAP Conf.*, Vienna, Austria, Aug. 2014, pp. 297-301.

[Samorodnitsky-94] G. Samorodnitsky and M. S. Taqqu, *Stable Non-Random Process*. New York, NY: Chapman and Hall / CRC, 1994.

[Servin-Aguilar-17] J. G. Servín-Aguilar, J. A. Pardiñas-Mir, and L. Rizo-Domínguez, "Breathing signal and sleep apnea detection using UWB technology," Internal Report *PhDEngScITESO-17-40-R*, ITESO, Tlaquepaque, Mexico, Nov. 2017.

[Servin-Aguilar-18] J. G. Servin-Aguilar, M. Muller, G. Abib, J. A. Pardiñas-Mir, and L. Rizo-Dominguez, "System to detect sleep apnea syndrome using the signal similarity," in *Int. Conf. Electrical, Electronics, Computers, Communication, Mechanical, and Computing (ECCMC)*, Tamil Nadu, India, Jan. 2018, pp. 1-6.

[Sriraam-08] N. Sriraam and C. Eswaran, "Performance evaluation of neural network and linear predictors for near-lossless compression of EEG signals", *IEEE Transactions on Information Technology in Biomedicin*e, vol. 12, no. 1, pp. 87-93, Jan. 2008.

[Stevenson-07] N. Stevenson, L. Rankine, M. Mesbah, and B. Boashash, "Modeling newborn EEG background using a time-varying fractional Brownian process," in *EUSIPCO Conf.*, Poznan, Poland, Sep. 2007, pp. 1426-1450.

[Taylor-00] J. D. Taylor, *Ultra-Wideband Radar Technology*. Boca Raton, FL: CRC Press, 2000.

[Varady-03] P. Varady, S. Bongar, and Z. Benyo, "Detection of airway obstructions and sleep apnea by analyzing the phase relation of respiration movement signals," *IEEE Transactions on Instrumentation and Measurement*, vol. 52, no. 1, pp. 2-6, Feb. 2003.

[Wang-15] Y. Wang, Y. Qi, J. Zhu, Y. Wang, G. Pan, X. Zheng, and Z. Wu, "A Cauchy-based state-space model for seizure detection in EEG monitoring systems," *IEEE Intelligent Systems*, vol. 30, no. 1, pp. 6-12, Jan. 2015.

[Waters-09] J. R. Waters and J. R. LaCourse, "Unconstrained and non-invasive respiration monitoring for obstructive sleep apnea prevention," in *IEEE 35th Annual Northeast Bioengineering Conference*, Boston, MA, May 2009, pp. 1-2.

[WHO-14] World Health Organization (2014. Nov. 03), *Chronic diseases and health promotion.* [Online]. Available: http://www.who.int/chp/en/.

[WHO-15] World Health Organization (2015, Jan, 29), *Datos interesantes acerca del envejecimiento* [Online]. Available: http://www.who.int/ageing/about/facts/es/.

[WHO-17] World Health Organization. (2017). *Obstructive Sleep Apnoea Syndrome (rev. Mar. 10)* [Online]. Available: http://www.who.int/respiratory/other/Obstructive_sleep_apnoea_syndrome/en.

[WHO-18] World Health Organization. (2018). *Epilepsy (rev. Mar. 18)* [Online]. Available: https://www.who.int/news-room/fact-sheets/detail/epilepsy.

[Yue-11] J. C. Yue, Y. Xu, E. Gunawan, E. C-P. Chua, A. Maskooki, Y. L. Guan, K-S. Low, C. B. Soh, and C-L. Poh, "Wireless sensing of human respiratory parameters by low-power ultrawideband impulse radio radar," *IEEE Transactions on Instrumentation and Measurement*, vol. 60, no. 3, pp. 928-938, Mar. 2011.

[Zhang-12] Z. Zhang and B.D. Rao, "Recovery of block sparse signals using the framework of block sparse bayesian learning", *ICASSP Conf.*, Kyoto, Japan, March 2012, pp. 3345-3348.

[Zhang-13a] W. Zhang, P. Passow, E. Jovanov, R. Stoll, and K. Thurow, "A secure and scalable telemonitoring system using ultra-low-energy wireless sensor interface for long-term monitoring in life science applications", *CASE Conf.*, Madison, WI, Aug. 2013, pp. 617-622.

[Zhang-13b] Z. Zhang, T-P. Jung, S. Makeig, and B.D. Rao, "Compressed sensing of EEG for wireless telemonitoring with low energy consumption and inexpensive hardware", *IEEE Transactions on Biomedical Engineering*, vol. 60, no. 1, pp. 221-224, Jan. 2013.

[Zhang-13c] Z. Zhang, T-P. Jung, S. Makeig, and B.D. Rao, "Compressed sensing for energy-efficient wireless telemonitoring of noninvasive fetal ECG via block sparse bayesian learning", *IEEE Transactions on Biomedical Engineering*, Vol. 60, pp 300-309, Feb. 2013.

Author Index

Subject Index